Naval Postgraduate School

Monterey, California

THESIS

MODIFICATION OF AN AQUILA UNMANNED AIR VEHICLE

by
John E.C. Stewart
March 1995

Thesis Advisor: Richard M. Howard
Second Reader: Conrad F. Newberry

Approved for public release; distribution is unlimited

1REPORT DOCUMENTATION PAGE

Form Approved OMB Np. 0704-

1. AGENCY USE ONLY *(Leave blank)*

2. REPORT DATE March 1995

3. REPORT TYPE AND DATES COVERED Master's Thesis

4. TITLE AND SUBTITLE MODIFICATION OF AN AQUILA UNMANNED AIR VEHICLE

5. FUNDING NUMBERS

6. AUTHOR(S) Stewart, John E.C.

7. PERFORMING ORGANIZATION NAME(S) AND ADDRESS(ES)
Naval Postgraduate School
Monterey CA 93943-5000

8. PERFORMING ORGANIZATION REPORT NUMBER

9. SPONSORING/MONITORING AGENCY NAME(S) AND ADDRESS(ES)

10. SPONSORING/MONITORING AGENCY REPORT NUMBER

11. SUPPLEMENTARY NOTES The views expressed in this thesis are those of the author and do not reflect the official policy or position of the Department of Defense or the U.S. Government.

12a. DISTRIBUTION/AVAILABILITY STATEMENT
Approved for public release; distribution is unlimited.

12b. DISTRIBUTION CODE

13. ABSTRACT *(maximum 200 words)*

The requirement exists at the Naval Postgraduate School Unmanned Air Vehicle Laboratory for an air vehicle capable of carrying a 60 pound payload. To that end, an air vehicle from the canceled Army Aquila program was modified to become the payload carrier. The modifications involved designing and building landing gear and an empennage. The landing gear design consisted of determining the anticipated loads and designing a structure to withstand those loads. The construction process was comprised of building the required molds, forming necessary components and, where possible, adapting existing items for use in the landing gear. The empennage design consisted of determining the unmodified air vehicle stability characteristics, determining the desired stability characteristics, determining the load acting on the empennage, and sizing the empennage to provide the desired characteristics and withstand the loads. The empennage construction process was comprised of cutting the required shapes, fashioning the required structural members, assembling the structure and fiberglassing the structure. The modified vehicle awaits an engine and other components required to make it operational.

14. SUBJECT TERMS Aquila, Unmanned Air Vehicle (UAV), Design, Fabrication

15. NUMBER OF PAGES 73

16. PRICE CODE

17. SECURITY CLASSIFICATION OF REPORT Unclassified

18. SECURITY CLASSIFICATION OF THIS PAGE Unclassified

19. SECURITY CLASSIFICATION OF ABSTRACT Unclassified

20. LIMITATION OF ABSTRACT UL

NSN 7540-01-280-5500

Standard Form 298 (Rev. 2-89)
Prescribed by ANSI Std. 239-18

Approved for public release; distribution is unlimited.

MODIFICATION OF AN AQUILA UNMANNED AIR VEHICLE

John E.C. Stewart
Lieutenant, United States Navy
B.S.A.E., University of Kansas, 1987

Submitted in partial fulfillment
of the requirements for the degree

MASTER OF SCIENCE IN AERONAUTICAL ENGINEERING

from the

NAVAL POSTGRADUATE SCHOOL

March 1995

Author: John E.C. Stewart

John E.C. Stewart

Approved by: Richard M. Howard

Richard M. Howard, Thesis Advisor

Conrad F. Newberry

Conrad F. Newberry, Second Reader

Daniel J. Collins

Daniel J. Collins, Chairman
Department of Aeronautics and Astronautics

ABSTRACT

The requirement exists at the Naval Postgraduate School Unmanned Air Vehicle Laboratory for an air vehicle capable of carrying a 60 pound payload. To that end, an air vehicle from the canceled Army Aquila program was modified to become the payload carrier. The modifications involved designing and building landing gear and an empennage. The landing gear design consisted of determining the anticipated loads and designing a structure to withstand those loads. The construction process was comprised of building the required molds, forming necessary components and, where possible, adapting existing items for use in the landing gear. The empennage design consisted of determining the unmodified air vehicle stability characteristics, determining the desired stability characteristics, determining the load acting on the empennage, and sizing the empennage to provide the desired characteristics and withstand the loads. The empennage construction process was comprised of cutting the required shapes, fashioning the required structural members, assembling the structure and fiberglassing the structure. The modified vehicle awaits an engine and other components required to make it operational.

TABLE OF CONTENTS

LIST OF SYMBOLS, ACRONYMS AND/OR ABBREVIATIONS

F.S.	Fuselage station
W.S.	Wing station
W.L.	Water line
α	Angle of attack
C_D	Coefficient of drag
C_L	Coefficient of lift
C_M	Pitching moment coefficient
C_N	Normal force coefficient
C_A	Axial force coefficient
X_{CP}	Longitudinal position of center of pressure, inches
$C_{l\alpha}$	Variation of rolling moment coefficient with angle of attack
$C_{M\alpha}$	Variation of pitching moment coefficient with angle of attack
$C_{y\beta}$	Variation of side force coefficient with sideslip angle
$C_{n\beta}$	Variation of yawing moment coefficient with sideslip angle
$C_{l\beta}$	Variation of rolling moment coefficient with sideslip angle
C_{lq}	Variation of rolling moment coefficient with pitch rate
C_{Mq}	Variation of pitching moment coefficient with pitch rate
$C_{L\dot{\alpha}}$	Variation of lift coefficient with rate of change of angle of attack
$C_{M\dot{\alpha}}$	Variation of pitching moment coefficient with rate of change of angle of attack
C_{lp}	Variation of rolling moment coefficient with roll rate
C_{yp}	Variation of side-force coefficient with roll rate
C_{np}	Variation of yawing moment coefficient with roll rate
C_{nr}	Variation of yawing moment coefficient with yaw rate
C_{lr}	Variation of rolling moment coefficient with yaw rate

ACKNOWLEDGMENT

To accomplish this project required more than I alone could muster. I would like to thank all that have helped. I must first thank my parents, James and June. It is from them I received my ambitions to undertake this task.

The beginning of this project progressed slowly. It was difficult to find information on the Aquila. To that end, I would like to thank Mr. Don Bane, of Lockheed Missiles & Space Company, Sunnyvale. He went out of his way and made several phone calls trying to locate the information I was interested in.

I would also like to thank Mr. William Drake, Jr. and Mr. Tom Johnson, both of Lockheed Missiles & Space Company, Santa Cruz. Mr. Drake was the resident expert on the Aquila program and gave me much insight into the program. Mr. Johnson went out of his way to copy relevant documents for my research.

The construction of the Blackbird was greatly influenced by Mr. Don Meeks, UAV Lab Technician. His attention to detail and personal interest in the project added significantly.

This project would not have existed except for the interest of Professor Rick Howard. To him I owe many thanks. His guidance brought me back on track when I had gone astray. His enthusiasm helped fuel my own during moments of despair. Thank you, Professor.

Finally, I must thank my wife, Lisa, and our three wonderful children, Kristine, John Jr. and Stephanie. Their support and understanding allowed me to complete this project. Their love kept me motivated.

I. INTRODUCTION

A. MISSION REQUIREMENT

Unmanned aerial vehicles (UAVs) have been in service since 1917 when Lawrence Sperry's "aerial torpedo" first flew for the US Navy. In the last 78 years, UAVs have undergone significant development [Ref. 1]. With the advent of Global Positioning Systems (GPS), advanced electro-optics, and electronic microminiaturization, UAVs have become an integral part of military operations.

The Israeli built Pioneer UAV, seen in Figure 1.1, is the current US deployed UAV. During Desert Storm, the Pioneer was utilized by the US Navy, US Army, and US Marine Corps. The Pioneer provided near-real time day or night reconnaissance, surveillance, target acquisition (RSTA), battle damage assessment (BDA), and battlefield management within line-of-sight of the ground control system. It performed these functions without personnel being shot down, killed or captured. [Ref. 2]

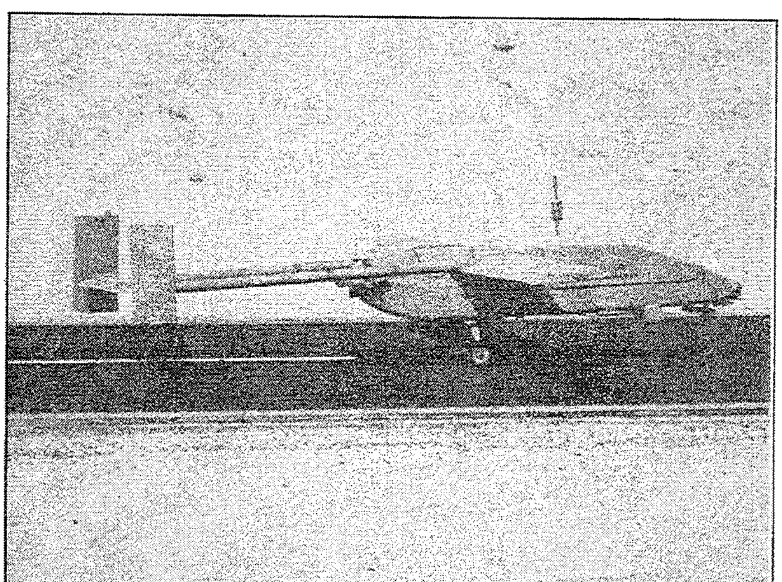

Figure 1.1 Pioneer Unmanned Aerial Vehicle From Ref [2]

The Navy used Pioneer from the battleships USS Wisconsin and USS Missouri, flying 151 sorties totaling 520 flight hours. The missions included RSTA, Naval Gunfire Support (NGFS), BDA, Maritime Interception Operations (MIO), and battlefield management. Examples of the Pioneer's effectiveness include the detection of two Iraqi patrol boats allowing for a strike to be directed on them. In a surveillance role, the Pioneer located two Silkworm antiship missile sites. The Pioneer allowed 320 ships to be identified. In addition, 64 sorties were flown providing NGFS for 83 missions. [Ref. 2]

The Pioneer provided a quick-fire link between real-time video and the shooters. The Pioneer operations validated the use of UAVs in the same airspace with manned aircraft and it provided the first successful integration of ship-based UAVs into combat operations. The Pioneer proved the requirement of UAVs in modern combat. [Ref. 2]

The Naval Postgraduate School has been developing and testing UAVs since 1987. The development and testing program provides military officers with the necessary background and skills to prepare them to supervise UAV and similar programs. In the development process, the need to test various systems in an airborne test bed has arisen time and again. The requirement exists for a payload-carrying platform to test various packages in a realistic environment. Although there are several vehicles available, a larger payload capacity is required.

B. OBJECTIVE

The Naval Postgraduate School Unmanned Air Vehicle Flight Research Laboratory (UAV FRL) acquired several items from the US Army's canceled Aquila program. With a gross takeoff weight of around 300 pounds and a payload capacity of 62 pounds, the Aquila airframe made an excellent candidate for a simple payload carrier. A problem arose when considering the launch and recovery of the vehicle. The original air vehicle did not have landing gear, as it was rail launched and recovered in a net. This method eliminated the need for a runway. Since no launch or recovery equipment was available, a more conventional method of launch and recovery was required. This facilitated the need for landing gear.

The Aquila was essentially a flying wing with a ducted propeller for propulsion. Because of this planform, the center of gravity was limited to one inch of travel. With the addition of landing gear and varying payload amounts, this restriction would require a large amount of ballast in certain configurations to ensure stability. Also, the original aircraft carried all its own flight control systems onboard, including a flight control computer and the required gyros. As a payload carrier, the aircraft would be controlled from the ground. These requirements necessitated the need for horizontal and vertical tail surfaces to increase the longitudinal and lateral-directional stability of the vehicle.

The project objective was to modify the existing airframe to provide the desired stability characteristics, yet maintain the portability of the modular aircraft. To perform this, the author had to first define the desired characteristics for the landing gear and an empennage. Then, based on the desired characteristics, the landing gear and empennage were designed and built. The modified air vehicle is designated the Blackbird, due to its original color. The original, unmodified air vehicle is shown in Figure 1.2.

To define the desired characteristics of Blackbird, the characteristics of the Aquila had to first be determined. The Aquila system was reviewed and used as a starting point for the design effort.

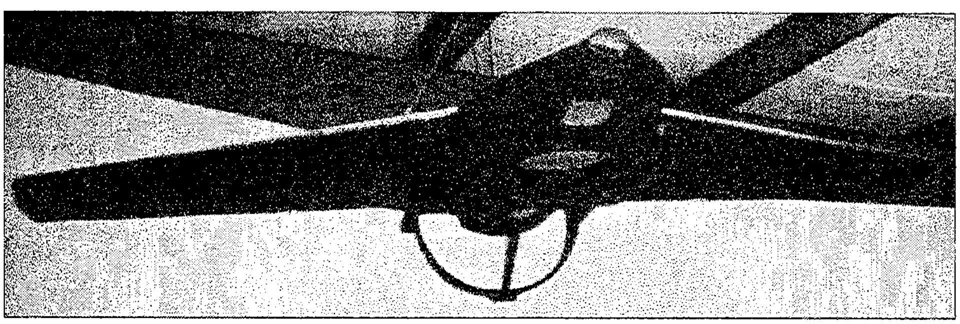

Figure 1.2 Unmodified Blackbird Air Vehicle

II. AQUILA PROGRAM

A. BACKGROUND

The Aquila program began in 1974 when the US Army opened bidding for a concept evaluation vehicle. Lockheed Missiles and Space Company (LMSC), of Sunnyvale, California, won the contract and began development. In December 1975, the XMQM-105 Aquila had its first flight. The Army awarded LMSC contracts for a target acquisition, designation and reconnaissance (TADAR) full scale development program which began on 31 August 1979. Under these contracts, Lockheed was to deliver 28 YMQM-105 Aquila air vehicles, along with the required ground control and support equipment.

The Aquila program was transferred from LMSC at Sunnyvale to Lockheed-Austin in mid-1983. During testing in January 1986, Aquila successfully demonstrated its capability to perform to its design specifications, and was used to designate tank targets for live Copperhead anti-tank rounds fired from artillery howitzers. Of the 310 test flights completed by January 1986, 306 were completely successful, 15 ended with parachute recoveries, and nine crashed. The second operational test was completed at Fort Hood, Texas, in spring of 1987. During this test 143 flights were conducted including the firing of 20 Copperheads and more than 150 rounds of other ammunition at the vehicles. Handoffs to other ground control stations were made at up to 28 miles. The US Army planned to purchase 376 air vehicles and 88 ground stations but in late 1987, the House Armed Services Committee canceled funding terminating the project. In parallel to Aquila, LMSC was developing Altair, an export version with a less expensive data link system. This project also died with Aquila.

In 1992, the Army released its residual Aquila assets to other DOD units. The Naval Postgraduate School UAV Lab obtained several parts including two fuselages, two wing sets, several propeller shrouds, a fuel bladder several propellers and a flight control computer. Although there were not enough parts to make a complete Aquila system, there were sufficient assets to create an air vehicle with considerable modifications.

B. AQUILA SYSTEM

The original Aquila system was designed to perform target acquisition, designation, aerial reconnaissance, and artillery adjustment missions. The small unmanned air vehicle including its mission payload was controlled from the ground control station and video imagery and target location information was returned via an antijam data link.

The system consisted of an air vehicle (AV), a ground control station (GCS), remote ground terminal (RGT), launch equipment, recovery equipment, and support equipment. The Aquila System is shown in Figure 2.1. [Ref. 3]

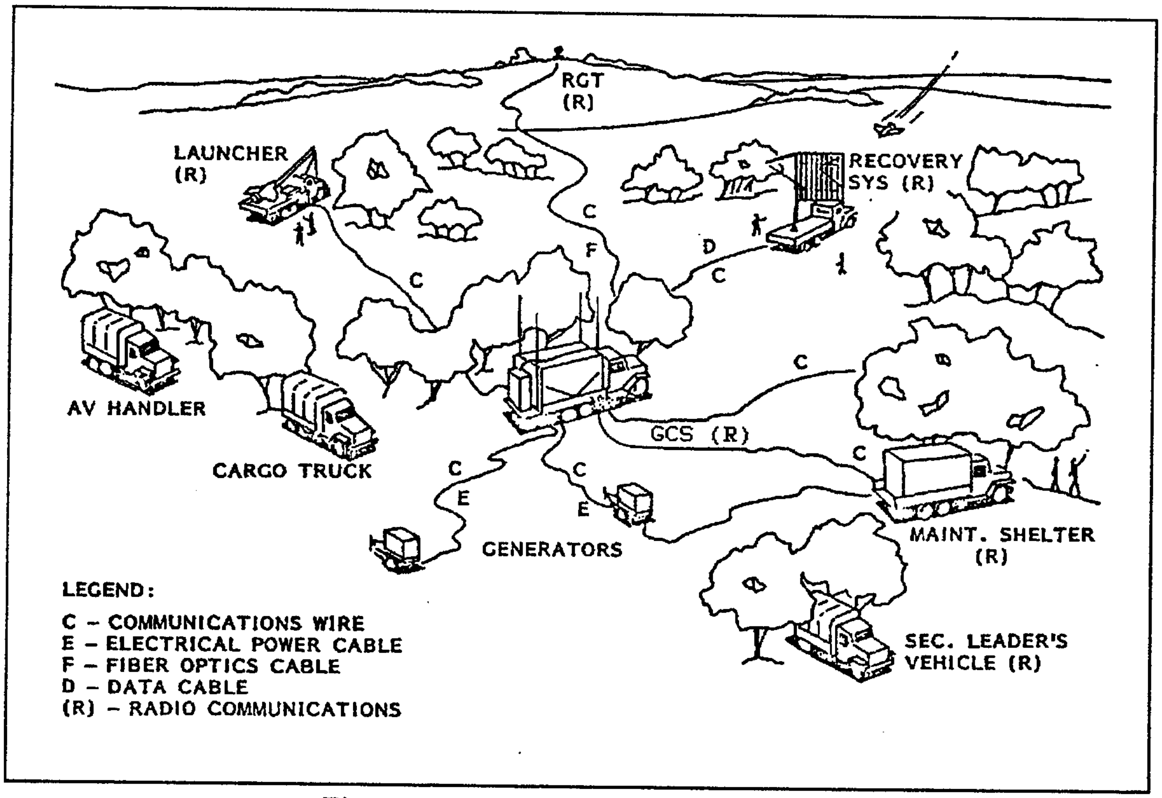

Figure 2.1 Aquila System From Ref [3]

The air vehicle consisted of an airframe, automatic flight controls, propulsion system, airborne data terminal (ADT), and mission payload subsystem. The airframe consisted of a fuselage with a propeller shroud assembly and two quick-disconnect wings constructed of a Kevlar/epoxy laminate. Some elements were reinforced using graphite/epoxy laminates. The fuselage housed the fuel system, flight control electronic package, attitude reference package, airspeed sensor, ADT system, engine and mission payload. The Aquila air vehicle layout is seen in Figure 2.2. [Ref. 3]

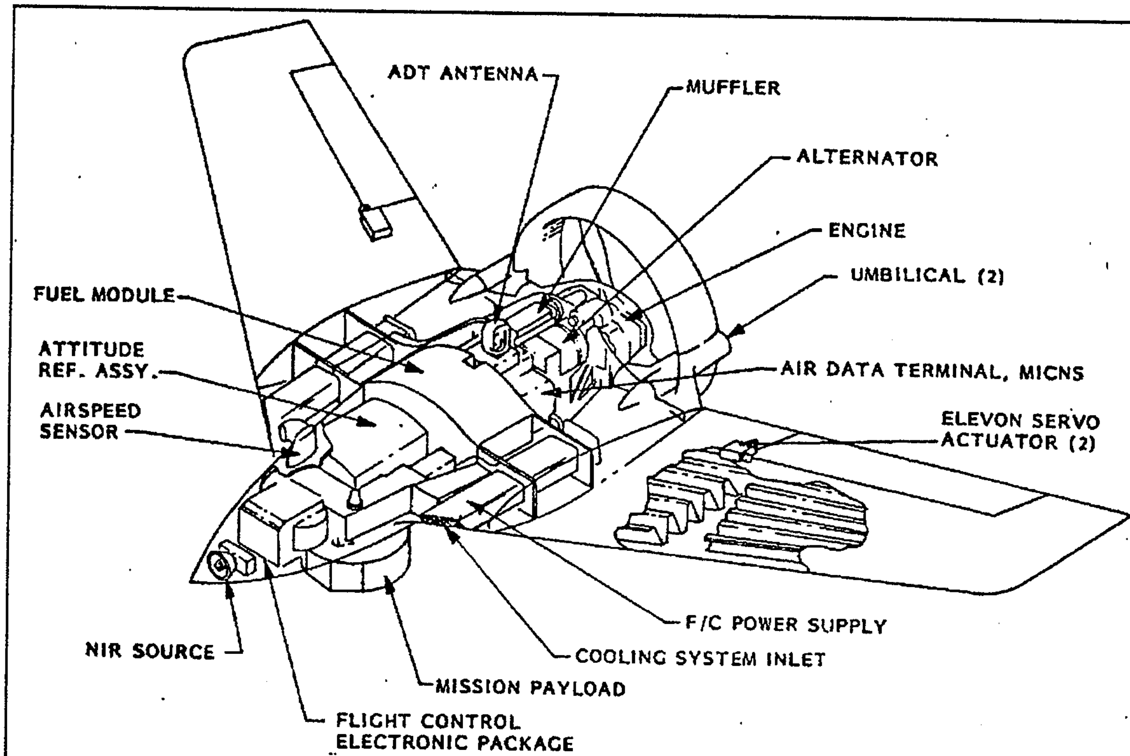

Figure 2.2 Aquila Air Vehicle From Ref [3]

The ground control station was the operation center and was housed in a mobile shelter. It included a mission planning facility, control and display consoles, computer and processing equipment, and tactical communications equipment. An All American Engineering HP-30 hydraulically actuated catapult mounted on a 5-ton truck catapulted the air vehicle into the air, see Figure 2.3. When the mission was complete, the AV was automatically guided to a truck-mounted Dornier vertical ribbon net, see Figure 2.4. Support equipment included ground power generators, an assembly and maintenance shelter, ground test equipment, trucks, trailers, and other equipment. [Ref. 3]

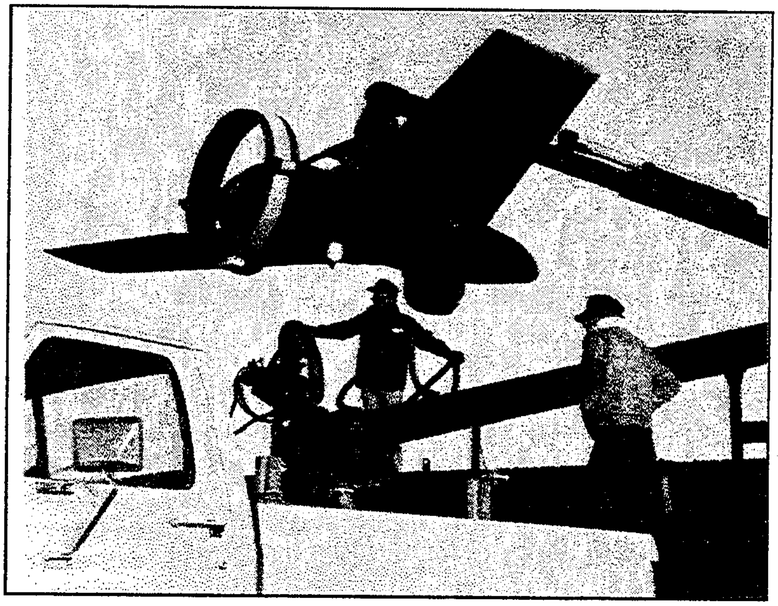

Figure 2.3 Aquila AV and Launch Vehicle From Ref [1]

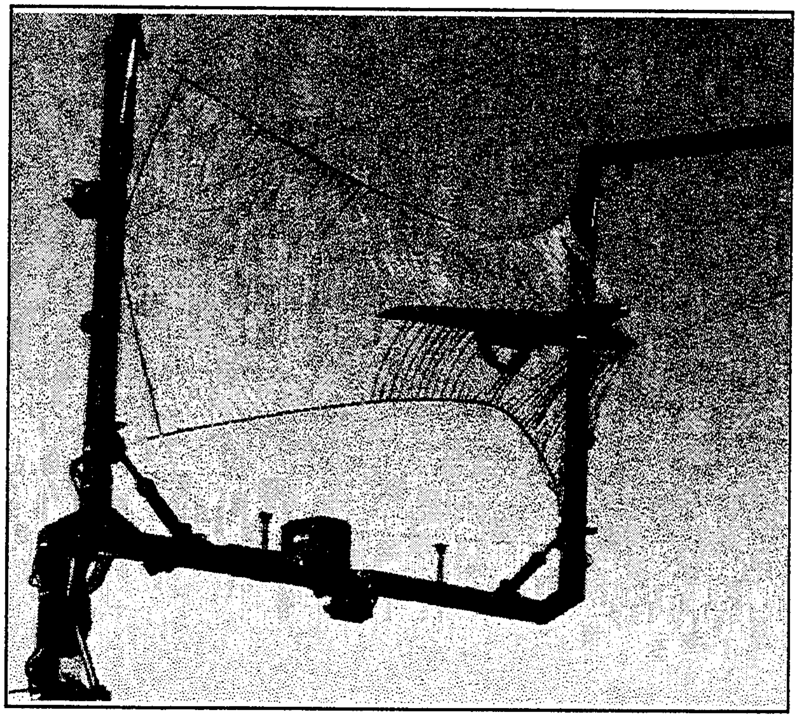

Figure 2.4 Aquila Net Recovery From Ref [1]

III. LANDING GEAR

A. DESIGN

The landing gear design process consisted of the following elements: estimating design loads, deciding on a general arrangement, and material selection.

1. Design Load Estimation

To estimate the design loads, several elements had to be determined or set. First, a weight and balance estimation was made. The empty fuselage, wing, and engine were weighed. This information was compared to the Aquila data from Lockheed. These weights agreed, so the Lockheed data was used for further estimations. Table 3.1 represents the Blackbird weight and balance estimation, based on the Aquila reference system

Type	Wt (lbs)	x (in)	W*x (in-lbs)	y (in)	W*y (in-lbs)	z (in)	W*z (in-lbs)
Wing	17.27	150.45	2598.3	0	0	1.31	22.6
Fuselage	35.45	140.04	4964.4	0	0	-1.54	-55
Main Gear	12	155	1860	0	0	-8	-96
Nose Gear	5	110	550	0	0	-8	-40
Engine	27.4	161.74	4431.7	0.69	18.91	0.64	17.5
Flight Controls	5	119.95	599.75	-2.1	-10.7	1.48	7.4
Electrical	2	144.32	288.64	-1.5	-3.02	0	0
Avionics/Link	0	147.79	0	-1.1	0	-0.15	0
Ballast	12	96	1152	0	0	0	0
Empennage	8	185	1480	0	0	6	48
Payload	60	122.2	7332	0.09	5.4	-4.05	-243
			xcg		ycg		zcg
Empty Weight	184.12		137.2		0.1		-1.8
Fuel	15	137	2055	0	0	1.6	24
			xcg		ycg		zcg
Take-Off Weight	199.12		137.2		0.1		-1.6
Fuel Used	15	139.1	2086.5	0	0	1.6	24
Landing Weight	184.12		137		0.1		-1.8

Table 3.1 Blackbird Weight and Balance Estimation

shown in Figure 3.1. Estimates were used for systems not included in the Aquila aircraft including the radio receiver, empennage and landing gear. The center of gravity (cg) was forced to the same position as the Aquila using ballast. This was done to keep the position of the cg relative to the wing aerodynamic center the same, allowing direct comparisons to be made between the Aquila and Blackbird dynamic responses.

With the take-off weight estimated, the landing loads had to be determined. There are two elements integral to determining landing loads: dynamic load and static load. To determine the dynamic load, a landing touchdown rate of five feet per second was used for the Blackbird. This compares to ten feet per second for full scale aircraft such as the P-3B, DC-9 and F-4E [Ref. 4]. Using half this value assumes the UAV will be able to absorb more of the air vehicle kinetic energy transmitted through the landing gear. This assumption is based on the fact that the Aquila was designed to withstand load factors of +/- 8 g's along the x, y, and z axes during parachute deployment. The kinetic energy of the vehicle was equated to the energy absorbed by the landing gear to determine required deflections. These calculations are shown in Appendix A. A static load factor of two was used in the design of the main gear.

2. General Arrangement

Simplicity in manufacture and operation was the main driving factor in the landing gear design. A tricycle, fixed landing gear arrangement was chosen to avoid the complications of retractable gear and due to the limited space within the vehicle for housing a retracted gear. A cantilever design was selected due to its simplicity in construction and incorporation to the existing airframe. The longitudinal position of the main gear in relation to the center of gravity was selected using the 15-degree tipback rule; the vertical position was determined to provide a 15-degree rotation angle before the shroud contacted the runway. These approximations were based on the methods of Reference 5 and are shown in Figure 3.1.

It was desired to take advantage of the modular properties of the vehicle to ensure ease of transport to and from the flying site. Maintaining the modular quality required keeping the main wheels as close to the W.S. 21.5 position as possible. To accomplish this goal and provide the necessary vertical distance, an inverted 'U' shape was selected. A computer spreadsheet program was used to determine the dimensions of the structure,. The gear structure was treated as a leaf spring main gear strut using the methods of Reference 6. The loads were input and the strut geometry was modified until the desired deflections were achieved. A simple finite element analysis was then performed to verify the deflections. Appendix B contains these calculations. After the design was constructed, testing revealed insufficient stiffness in the vertical portions of the struts. To rectify this problem, a support strut was added. The final design is shown in Figures 3.2 and 3.3.

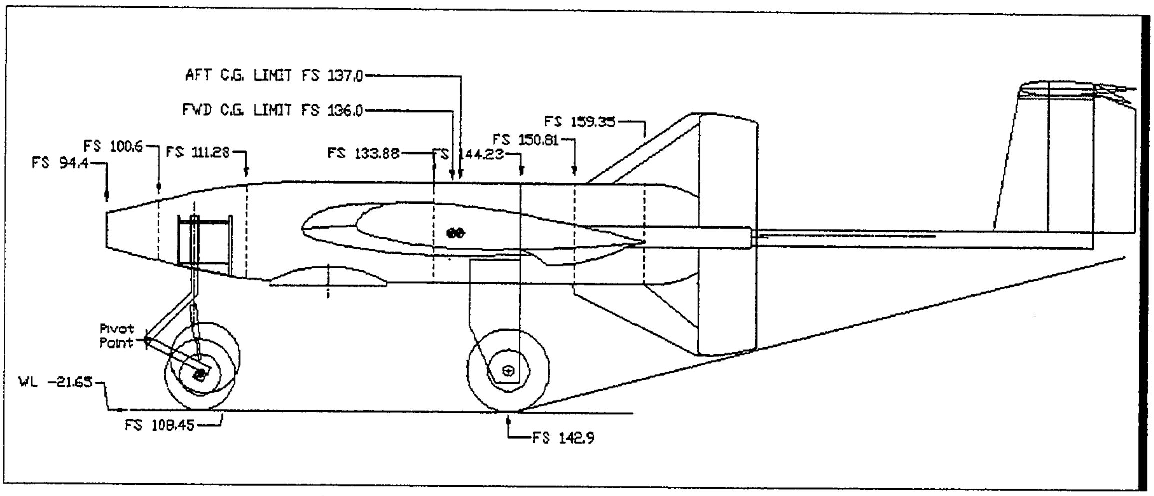

Figure 3.1 Landing Gear Position Criterion

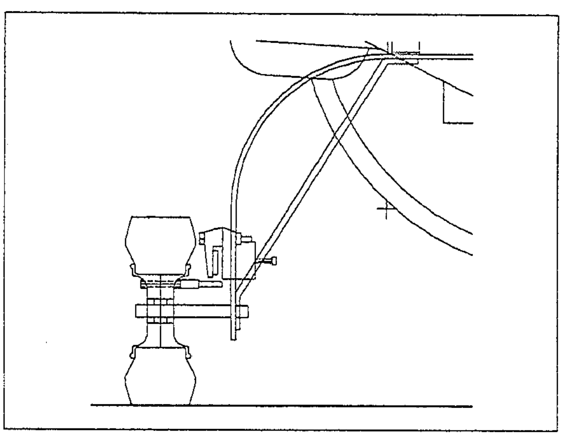

Figure 3.2 Main Gear Front View

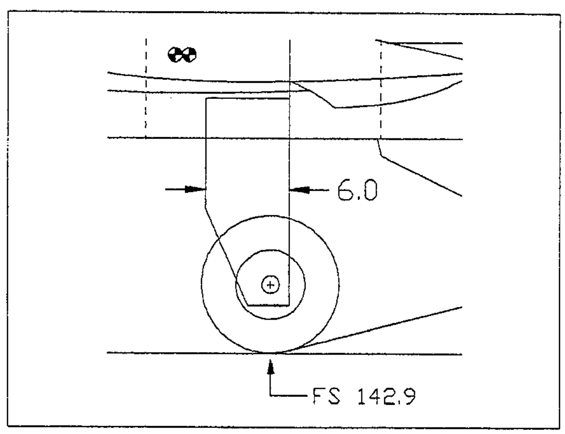

Figure 3.3 Main Gear Side View

A previously purchased set of wheels was utilized for the landing gear. The wheels were 4-inch Azusalite Nylon wheels with integral roller bearings that required a 5/8-inch axle. These wheels have applications including homebuilt and ultralight aircraft. In addition, 4.10/3.50-4 size tires were mounted on the wheels. These tires were used for the main landing gear, but a smaller, 2.80/2.50- 4 tire was used for the nose gear.

In consideration of the size of the Blackbird, the decision was made to put brakes on the main wheels. This feature would provide the ability to fly from shorter runways and would enhance safety by making the vehicle more controllable on the ground. Initially, a brake assembly was designed, but the design was discarded in favor of a commercial brake assembly that could be adapted to the air vehicle. Mechanical go-cart brakes were used with special aluminum rotors. The wheel and brake mount is shown in Figure 3.4.

The nose gear was designed to provide adequate steering ability while dampening out transient loads due to uneven terrain. The structure was designed to be strong enough to withstand normal landing loads, but in the event of excessive loads, the nose gear assembly would fail before doing irreparable damage to the air vehicle. The reasoning was that another nose gear assembly could be constructed more easily than another air vehicle. A pivoting arm assembly with a spring/shock absorber was used. The design is presented in Figures 3.5 and 3.6.

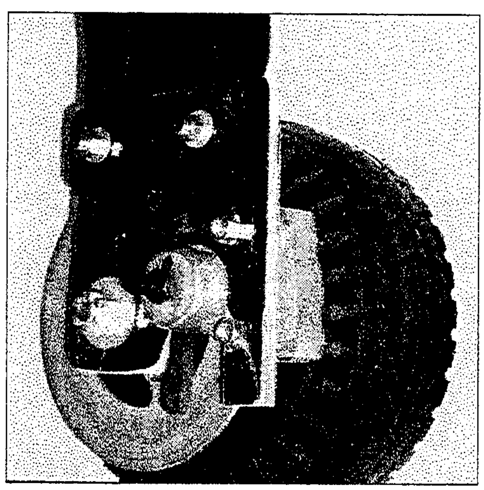

Figure 3.4 Wheel/brake Assembly

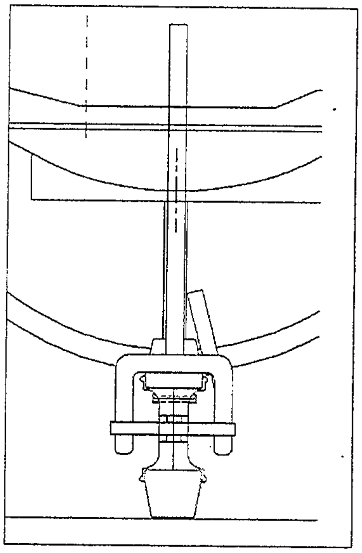

Figure 3.5 Nose Gear Front View

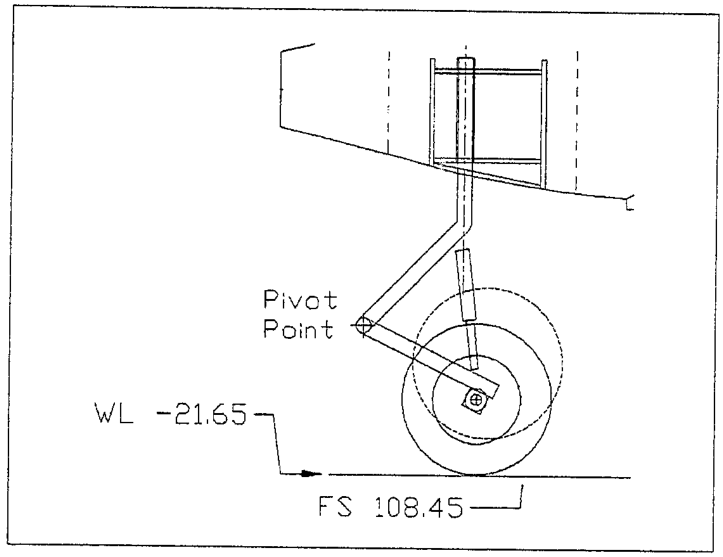

Figure 3.6 Nose Gear Side View

Based on the main gear position, the parachute mounting brackets used on the Aquila for the backup parachute recovery system were chosen as mounting points. These brackets provided a sturdy mounting surface able to withstand landing loads and transmit them through the fuselage structure. The nose mounting position was more difficult to select. Although there was a structural bulkhead at F.S. 106, this position was too far aft for the aircraft to meet the 55-degree tip-over criterion given in Reference 4. The lateral tip-over criterion is shown in Figure 3.7. To meet the criterion, a box structure was selected, supported on either end by bulkheads mounted to the side structure.

3. Material Selection

The two options for main gear construction material were aluminum and fiberglass/epoxy composite. With the unusual shape of the gear, and to take advantage of the high strength-to-weight ratio, a fiberglass/epoxy composite structural material was selected. Fiberglass/epoxy lay-ups had been used on other flight lab vehicles and, therefore, represented a known structural material.

For the nose gear, weight was not an issue. Although it is almost always desirable to keep aircraft component weight down, this was not the case for the Blackbird nose gear.

Since the weight and balance estimate required approximately 12 pounds of ballast in the nose, some of that weight could be provided by the nose gear. Another, more influential factor, was the availability of materials. Aluminum tubing of sufficient strength was available, but fittings to assemble the gear would have to be manufactured specially. Due to time constraints, the tubular construction approach was discarded. Schedule 40, 6061-T6 aluminum pipe with a nominal diameter of ½-inch was chosen for the nose gear assembly. The pipe provided the strength required along with simplicity in construction and the material was readily available locally. Aluminum pipe fittings were used with some modifications.

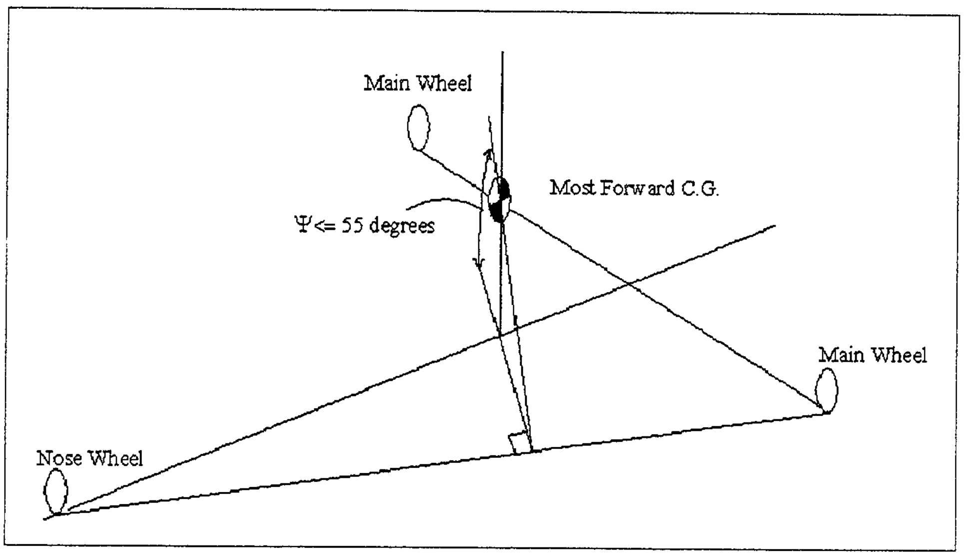

Figure 3.7 Lateral Tip-over Criterion

B. CONSTRUCTION

1. Main Landing Gear

The main landing gear strut assembly was constructed using wet fiberglass/epoxy lay-ups. First, a mold was required. This mold was constructed from a series of 4 foot by 4 foot plywood sheets. These sheets were glued together to form a 4x4 foot block approximately 8 inches thick. On this block, the desired landing gear dimensions were laid out and then cut out using a band saw. The inside section of the male mold was unnecessary and therefore removed to lighten the mold.

Analysis indicated a thickness of 0.30 inches of a fiberglass/epoxy lay-up would provide sufficient stiffness to support the vehicle. Thirty layers of 9-ounce cloth were used in the construction. The male mold was covered by a sheet of Mylar. The first layer of fiberglass cloth was laid upon the Mylar and saturated with resin. Then the next sheet was laid down. This process was repeated until all thirty layers had been positioned. Then another sheet of Mylar was placed over the lay-up and the female portion of the mold was put on top the assembly. The mold and fiberglass lay-up are shown in Figure 3.8.

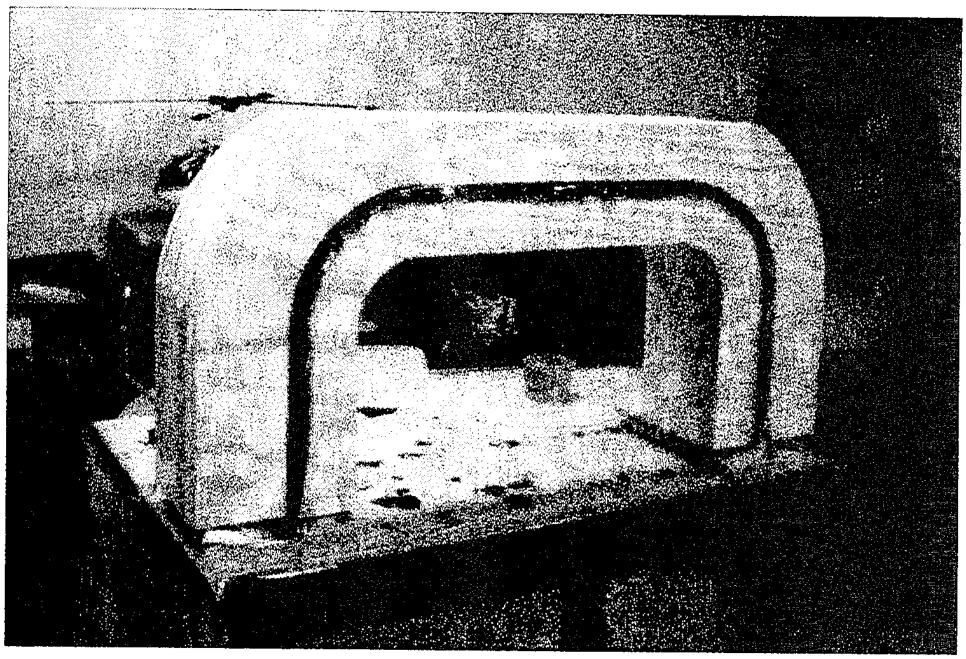

Figure 3.8 Main Landing Gear Mold and Lay-Up

The lay-up was allowed to cure for four days. The mold was then taken apart revealing the desired part, seen in Figure 3.9. This part was then cut and shaped into the final desired piece.

2. Nose Landing Gear

The nose gear assembly began with the construction of mock-ups. These mock-ups were useful to visualize the function of the gear and to identify and eliminate any problems.

The pipe was cut into the desired sections using a pipe cutter. These sections were then threaded and screwed into the pipe fittings. The pivot point was fashioned using a 'T' fitting machined to accommodate a set of Delrin bushings. The brackets for mounting the axle were machined from aluminum stock and heli-arc welded to the supports. The entire assembly was then screwed together. To prevent inadvertent unscrewing of the parts, holes were drilled in each connection and set screws were tapped into place. The final nose gear assembly is shown in Figure 3.10.

Steel bolts of 5/8-inch diameter were used as the axles for the main wheels while a 5/8-inch threaded steel rod was used for the nose wheel. Set collars hold the wheels on the axles while castle nuts hold the axles in place.. The final assembly is shown in Figure 3.11.

Figure 3.9 Unfinished Main Landing Gear Strut

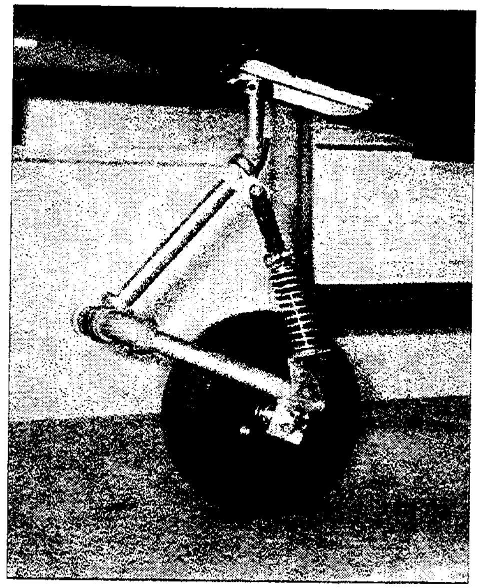

Figure 3.10 Nose Landing Gear

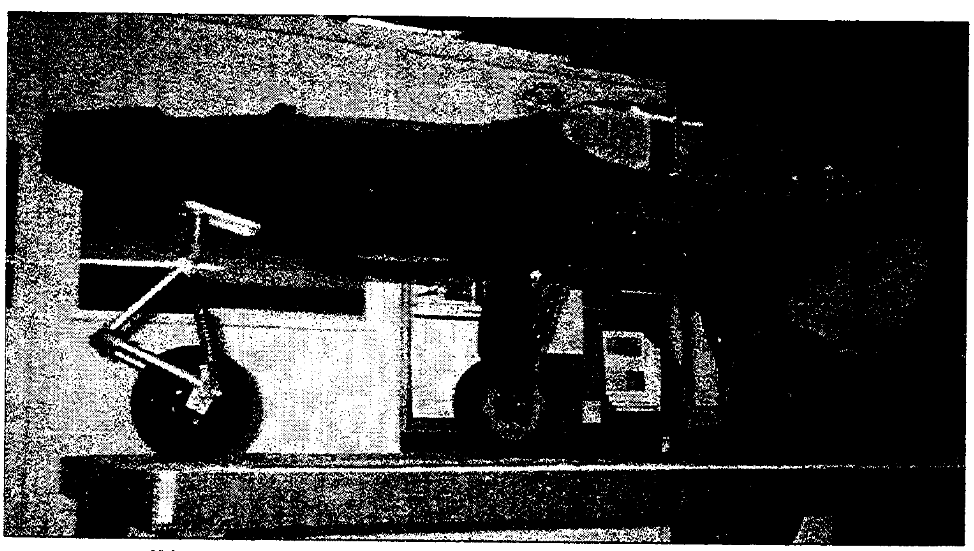

Figure 3.11 Blackbird with Complete Landing Gear

IV. EMPENNAGE

A. DESIGN

The main purpose of the empennage was to ensure handling qualities desired for a ground-controlled aircraft. The aircraft needed sufficient longitudinal and lateral-directional stability to allow it to remain in a trim condition if the pilot took his eyes from it for a moment. To achieve this, goals had to be set. Handling qualities for radio controlled aircraft had not been set by any agency known to the author. To develop a set of handling qualities, the air vehicle was treated as a scale aircraft and the military aircraft handling qualities were applied with some modification.

The particular handling qualities of concern were the short period, the Dutch-roll response and the spiral response. Although information on the XMQM-105 Aquila's dynamic characteristics was available, no such data were available for the YMQM-105, the modified airframe. Appropriate dynamic characteristics were estimated as described below.

It was desired that the aircraft handle like a transport or light general aviation aircraft. The vehicle was to be heavily damped in the short period mode, have a fairly large spiral time to double and exhibit a well damped Dutch-roll response. It was assumed that the Aquila was a 1/3-scale aircraft. This gave the following values for the "full size" aircraft [Ref. 7].

	Scale factor: 1	Scale factor: 3
Wing Span	11.5 ft	34.5 ft
Weight	200 lbs	5400 lbs
Power shp	28 shp	1309.43 shp

Table 4.1 Scale Factor Comparisons

The damping ratios were not scaled. The dynamic goals are given in Table 4.2. Once goals were established, the empennage design was initiated.

Dynamic Parameter	Full Scale		Aquila	
Short Period	$3 < w_n < 10$	$0.3 < \zeta < 2.0$	$5.2 < w_n < 17$	$0.3 < \zeta < 2.0$
Dutch Roll	min $w_n = 1.0$	min $\zeta = 0.19$	min $w_n = 1.7$	min $\zeta = 0.19$
Spiral (minimum time to double)	20 sec		11.55 sec	

Table 4.2 Dynamic Parameter Comparisons

1. Horizontal Tail

a. Sizing

To determine the physical characteristics of the horizontal tail, the methods of Reference 9 were utilized. First, the longitudinal position of the horizontal tail was estimated. The mean aerodynamic center of the horizontal tail was put at FS 208. This position provided a maximum moment arm for the tail while keeping the end of the boom within the 15-degree rotation angle constraint. The vertical position of the horizontal tail was also fixed. To avoid any power/elevator coupling, the horizontal tail was placed such that it was outside the propeller slipstream. This positioning would eliminate the need to adjust the elevator with power changes. That aspect is most important during landing where large power changes are required. A NACA 0012 airfoil was used on the horizontal tail in concurrence with other aircraft design.

After fixing these values, the tail volume coefficient and aspect ratio were varied and examined. A Matlab script file was written to estimate the nondimensional longitudinal derivatives based on varying the horizontal tail volume and aspect ratio. These derivatives were used to find the dimensional derivatives and the short period response. The output of the code is shown graphically in Figures 4.1 through 4.3. The code is contained in Appendix C.

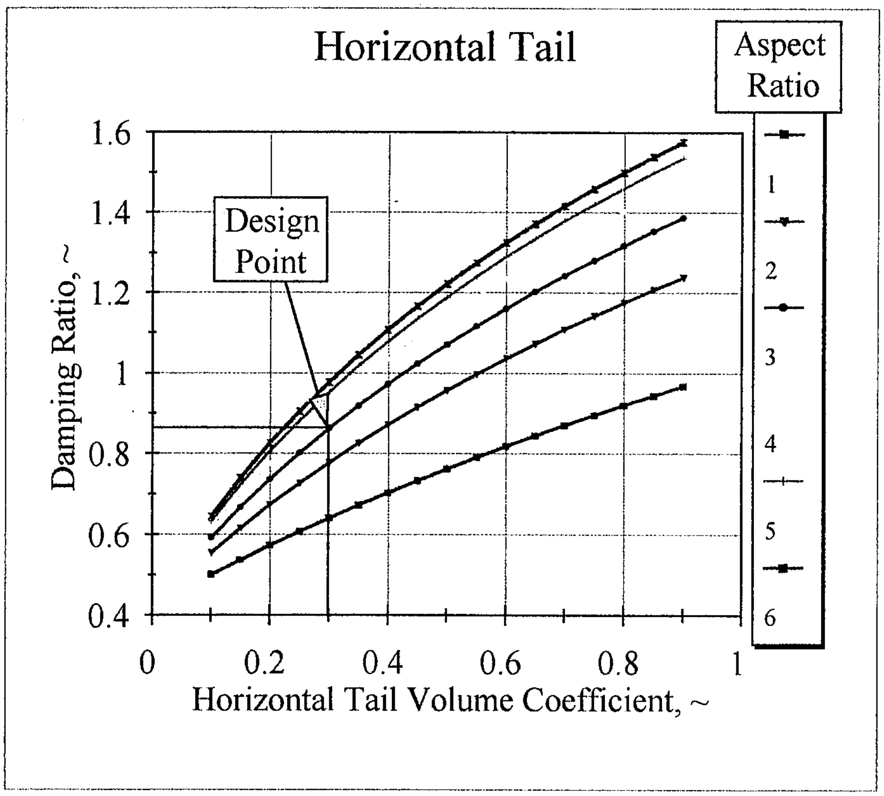

Figure 4.1 Damping Ratio vs Tail Volume Coefficient

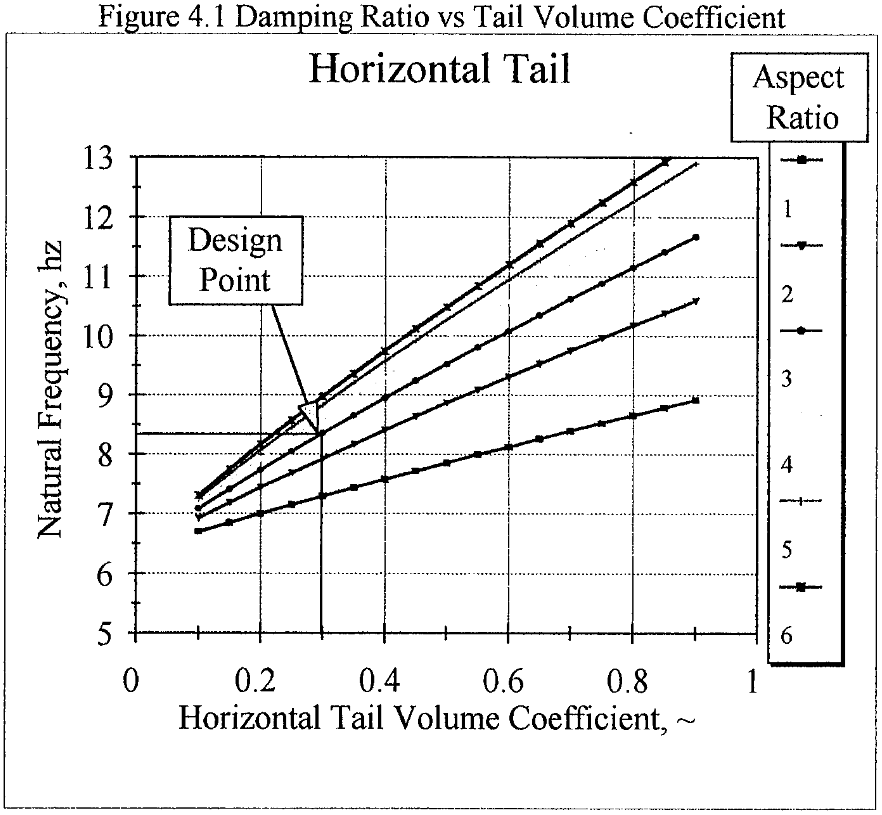

Figure 4.2 Natural Frequency vs Tail Volume Coefficient

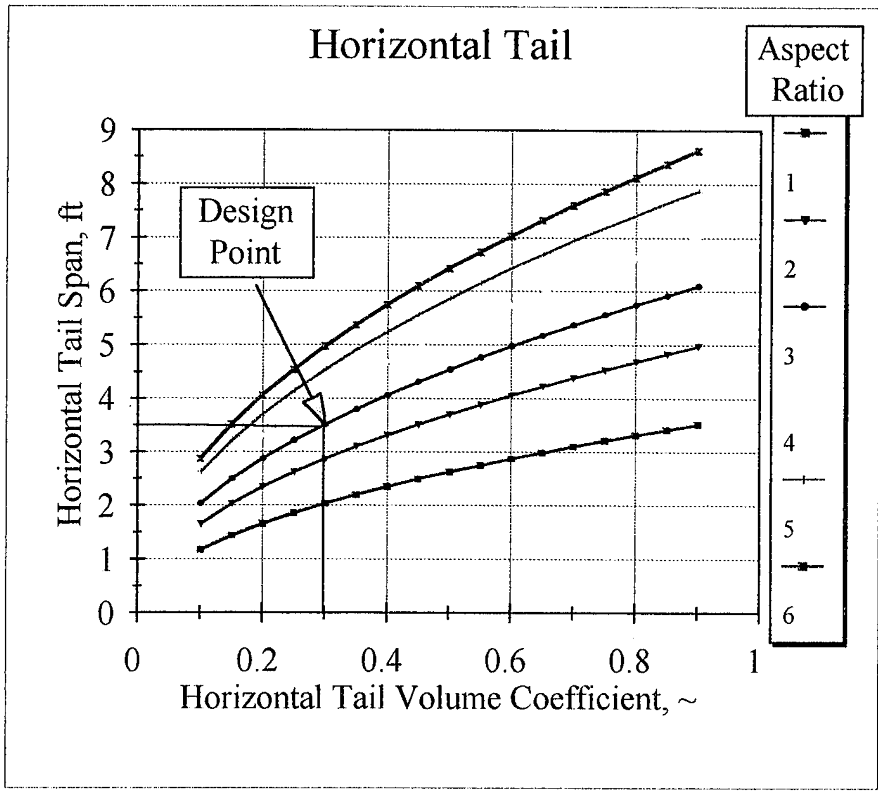

Figure 4.3 Horizontal Tail Span vs Tail Volume Coefficient

A tail volume coefficient was assumed and the range of aspect ratios was investigated. It was desired to maintain the modular nature of the vehicle. That desire limited the span of the horizontal tail to approximately 41 inches. A final span of 42 inches with an aspect ratio of three was finally decided upon. This result was based on a horizontal tail volume coefficient of 0.3.

The elevator was sized by comparing several general aviation aircraft elevator chords. The elevator chords were typically 30 to 40 percent of the horizontal tail chord. A value of 35 percent was used for the Blackbird. To verify sufficient control power, the aircraft data was entered into the Digital Datcom program, provided by Air Force Flight Dynamics Laboratory at Wright-Patterson Air Force Base [Ref. 8]. The output from this code is presented in Appendix D.

The horizontal tail was to originally have a leading edge sweep comparable to that of the wing. It was later determined a straight, non-tapered horizontal tail would be more desirable since the straight tail would be easier to construct. A planform view of the final design is presented in Figure 4.4.

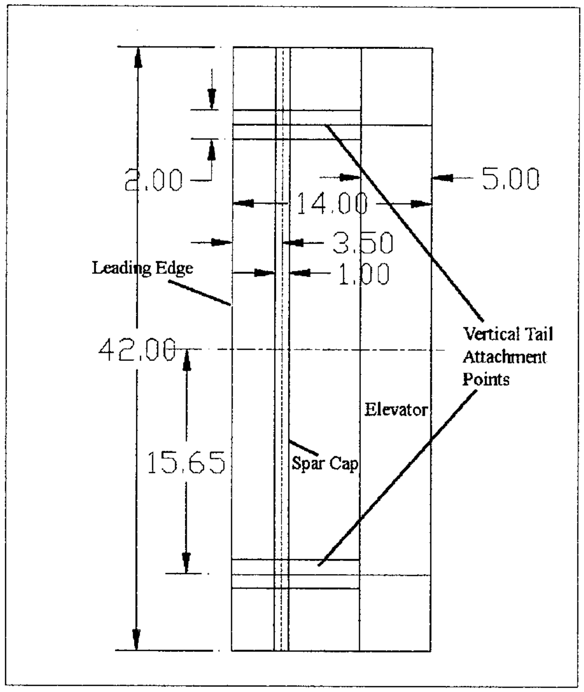

Figure 4.4 Horizontal Tail Planform

b. Structure

To size the horizontal tail structure, a maximum design load had to be determined. A flight condition of 12 degrees angle of attack at 120 knots was chosen. The load was determined using a maximum elevator deflection of 20 degrees. The total load was calculated to be 314 pounds. This load was distributed across the span of the horizontal tail and the reactions at the intended mounting points were determined. Then the shear and moment diagrams were developed by numerically integrating the load diagram. Using the maximum moment and the methods of Reference 9, the spar caps were sized. A 1/4-inch balsa wood spar cap with a layer of 3-ounce fiberglass cloth was used.

2. Vertical Tail

With the horizontal tail designed, the vertical tail design was simple. The vertical tail size was driven by the fact the vertical tail had to support the horizontal tail. To provide a smooth joining surface, a tip chord of 14 inches was chosen. An NACA 0012 airfoil was also used for the vertical tail. To ensure a smooth connection with the supporting booms, a root chord of approximately 17 inches was required. This root and tip chord combination corresponded with a leading edge sweep of 10 degrees. The final design is presented in Figure 4.5.

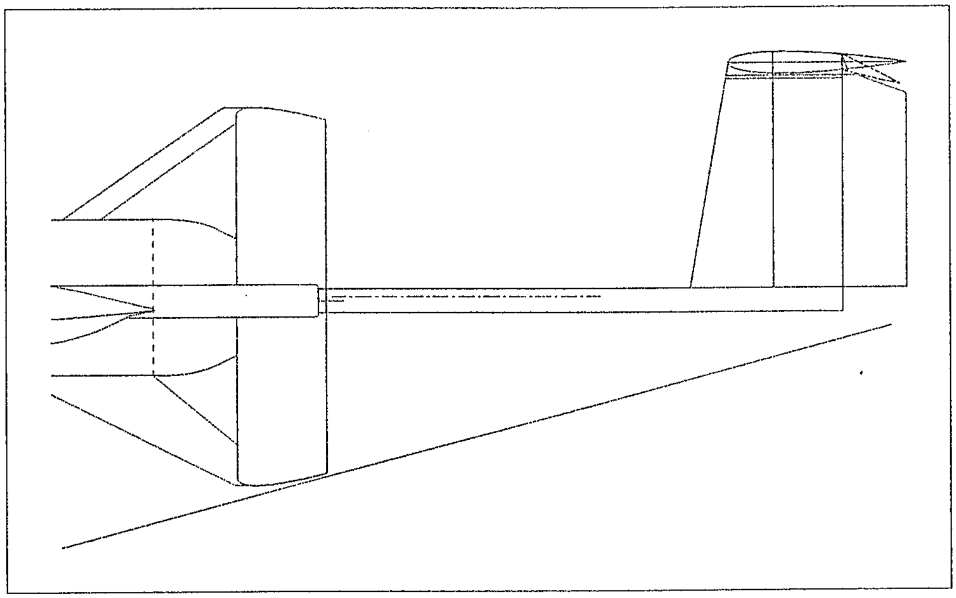

Figure 4.5 Vertical Tail and Boom Assembly

3. Tail Booms

On either side of the propeller shroud are tubular supports. The decision was made early in the design to use these supports as mounting points for the tail booms. This limited the maximum diameter for the tail booms. A number of commercially available aluminum booms were considered. The maximum horizontal tail load was used to size the booms. The aluminum yield strength values were taken from Reference 11. Each boom needed to withstand 157 pounds. Using this load, the maximum moment was determined and a spread sheet program was used to compare the weight and the yield strength of the candidate tubes [Ref. 12]. These results are presented in Figures 4.6 and 4.7. The table relating the configuration number to the actual size is given in Appendix E. Based on the analysis and local availability, a 2-inch diameter, 0.065-inch thick 6061-T6 aluminum tube was used for both booms.

B. CONSTRUCTION

For simplicity of construction and exceptional strength, a foam/fiberglass construction method was used for the tail surfaces.

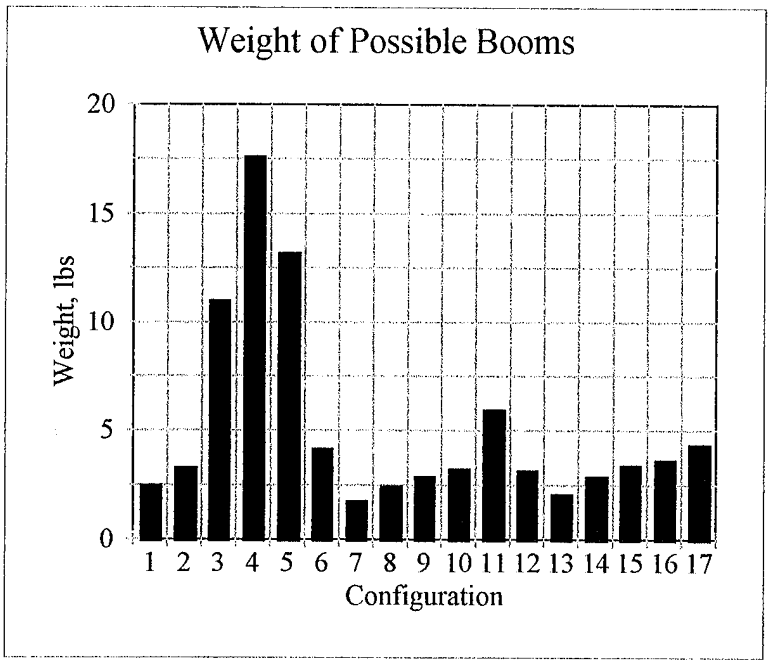

Figure 4.6 Boom Candidate Weight Comparison

1. Horizontal Tail

The horizontal tail was cut from closed cell foam using a hot wire. Airfoil templates were made from Formica and attached to foam blocks of the desired semispan. Then an electrically-heated wire was used to cut through the foam along the edge of the template. The resulting sections were glued together using a structural epoxy adhesive. A pair of vertical-tail-mounting interfaces was formed from balsa wood blocks. Slots were cut into

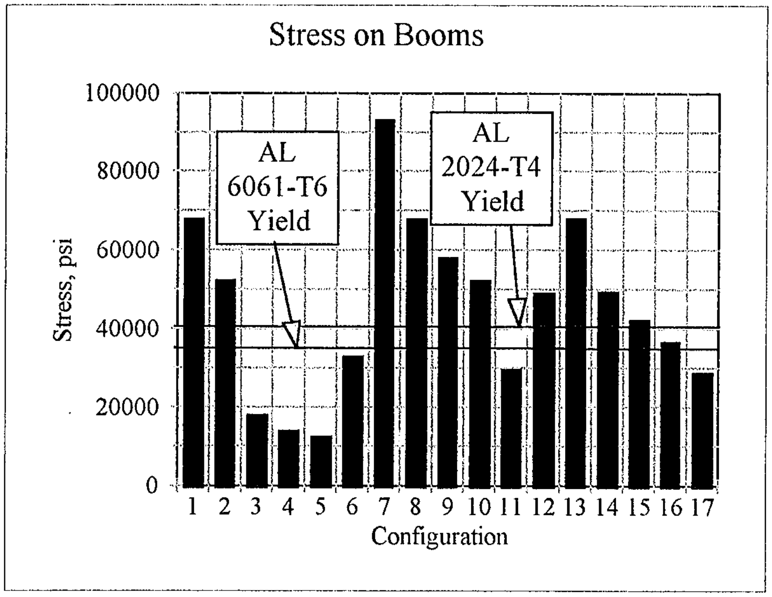

Figure 4.7 Boom Candidate Yield Stress Comparison

the tail and these interfaces were glued into place. A groove was then cut to accommodate the spar caps using a Dremel Tool with a router attachment. The spar caps were then epoxied into place. Tip sections were cut from balsa and glued into place. To provide a smooth surface for the fiberglass, the imperfections were filled using vinyl spackle. The surface was sanded and then glassed using 6-ounce fiberglass. The final horizontal tail is shown in Figure 4.8.

2. Vertical Tail

The vertical tail construction technique was similar to that of the horizontal tail. The foam sections were cut using a hot wire. The roots were then sanded into the shape of the booms to ensure a smooth transition from the boom to the vertical tail. The foam sections were then glued to the booms. To connect the horizontal tail to the vertical tail, some substantial structure other than foam was required. Balsa tips were fashioned and anchor nuts were placed inside the tips. These tips were then glued to the vertical tails. The assembly was then covered in 6-ounce glass. To add to the structural strength, a 2-inch strip of carbon fiber was laid up wet with the fiberglass.

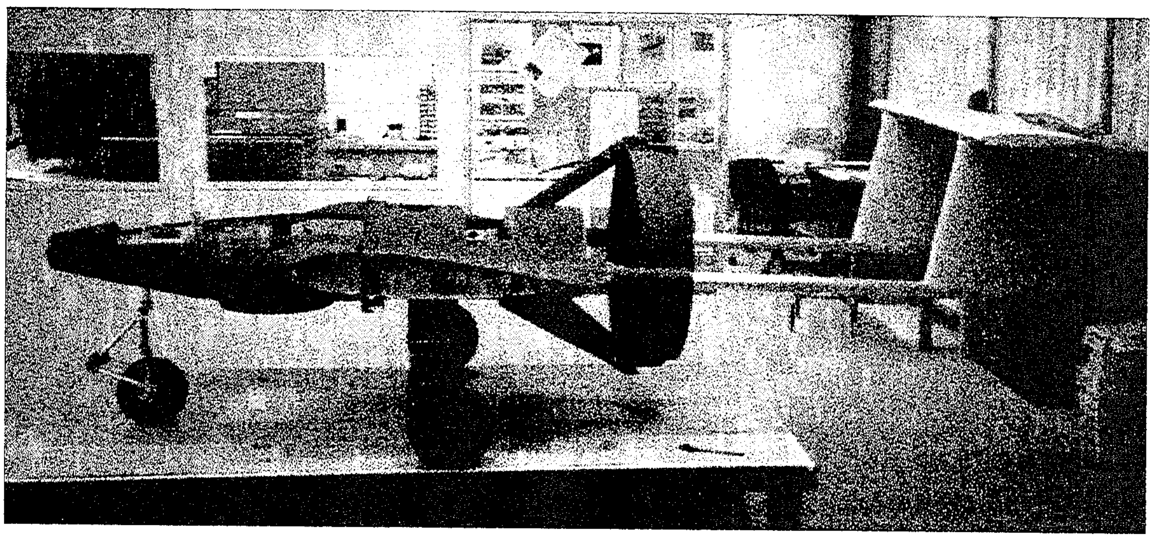

Figure 4.8 Modified Blackbird

V. SUMMARY

An air vehicle from the canceled Army Aquila program was modified to produce a payload carrier. The modifications involved designing and building both landing gear and an empennage. The landing gear design consisted of determining the anticipated loads and designing a structure to withstand those loads. The construction process was comprised of building the required molds, forming necessary components and, where possible, adapting existing items for use in the landing gear. The empennage design consisted of determining the unmodified air vehicle stability characteristics, determining the desired stability characteristics, determining the load acting on the empennage, and sizing the empennage to provide the desired characteristics and withstand the loads. The empennage construction process was comprised of cutting the required shapes, fashioning the required structural members, assembling the structure and fiberglassing the structure.

VI. RECOMMENDATIONS

Although a large portion of the Blackbird modification has been completed, there still exist several issues which must be addressed prior to flight testing. Below is a list of items yet to be completed: control surfaces, engine mounting, radio and servomotor installation, and taxi tests.

A. CONTROL SURFACES

The empennage control surfaces have already been sized. They need to be cut from the existing structure and have hinges attached. The elevator was originally intended to be split into two sections, each controlled by a separate servo. This reduces the size of the required servo and adds a safety factor by introducing redundancy to the pitch control system.

B. ENGINE MOUNTING

Although the original Aquila engine is not available, there is an alternative. The UAV FRL possesses similar engines which can be used. These two-stroke, two-cylinder, air-cooled 22-HP engines have been run and tested with other projects. What is required is the design and manufacture of a proper engine mounting system similar to that used on the original airframe, and the fitting of available Aquila propellers to the driveshaft.

C. RADIO AND SERVO INSTALLATION

The UAV FRL has several RC receivers and servos of different sizes. Mounting fittings need to be installed and the proper size servos put in place. It was estimated that 1/4-scale servos would suffice for the elevators and rudders. A larger servo is available for the nose wheel steering and brakes. Original Aquila elevon servos are available but would have to be adapted to interface with the RC receiver. The Aquila servos are analog and an analog-to-digital converter is required to allow the receiver to communicate with the servo. It may be possible to use the original Aquila servos to control other functions as well. In addition to radio and servo mounting, an electrical system must be installed to support the RC system. The engines have small generators on them which could be used to continuously charge a series of batteries. The batteries could be placed in the nose of the aircraft to eliminate the need for some of the ballast.

D. TAXI TESTS

Prior to any flight tests, taxi tests should be performed. The initial tests should be conducted without the engine operating to test the brakes and ground controls. Then, slow speed taxi tests should be performed to allow the operator to become familiar with the handling characteristics of the vehicle. The natural progression of testing would lead to high speed taxi tests and eventually to flight testing.

LIST OF REFERENCES

1. Munson, Kenneth, *World Unmanned Aircraft*, Jane's Publishing Company Limited, London, 1988.

2. Raach, George T., et. al., *Conduct of the Persian Gulf War*, U.S. Government Printing Office, Washington, D.C., 1992.

3. Tosch, N.G., et. al., *Army RPV Systems Project Mock-Up Review Report*, Lockheed Missile & Space Company, Sunnyvale, CA, 1980.

4. Roskam, J., *Airplane Design: Part IV: Layout Design of the Landing Gear and Systems*, Roskam Aviation and Engineering Corp., Ottawa, KS, 1986.

5. Roskam, J., *Airplane Design: Part II: Preliminary Configuration and Integration of the Propulsion System*, Roskam Aviation and Engineering Corp., Ottawa, KS, 1985.

6. Thurston, D.B., *Design for Flying*, McGraw-Hill Book Company, New York, 1978.

7. Hall, S., "Dymnamic Modeling", <u>Sport Aviation</u>, pp. 30-35, July 1987.

8. Air Force Technical Report AFFDL-TR-79-3032, Volume I, *The USAF Stability and Control Digital Datcom: Volume I, Users Manual*, 1979.

9. Roskam, J., *Airplane Design: Part VI: Preliminary Calculation of Aerodynamic, Thrust and Power Characteristics*, Roskam Aviation and Engineering Corp., Ottawa, KS, 1987.

10. Hollman, M., *Modern Aircraft Design*, Martin Hollman, Monterey, CA, 1986.

11. Allen, D.H., Haisler, W.E., *Introduction to Aerospace Structural Analysis*, John Wiley & Sons, New York, 1985.

12. Stoney, R.B., Design, *Fabrication and Test of a Vertical Attitude Takeoff and Landing Unmanned Air Vehicle*, Naval Postgraduate School, Monterey, CA, 1993.

13. Smith, H.W., *Aerospace Structures: Matrix Analysis*, University of Kansas, Lawrence, KS, 1985.

14. Roskam, J., *Methods for Estimating Stability and Control Derivatives of Conventional Subsonic Airplanes*, Roskam Aviation and Engineering Corp., Ottawa, KS, 1983.

15. Patrick, J., *Low Speed Wind Tunnel Test to Obtain Air Vehicle Aerodynamic Data for Analysis of Flight Performance, Stability, and Control, to Calibrate Air Data Sensors, and to Obtain Propeller Thrust and Power of the Aquila RPV*, Lockheed-Georgia Company, Marietta, GA, 1983.

APPENDIX A: MAIN LANDING GEAR LOAD CALCULATIONS

The sink rate was used to determine the amount of energy to be absorbed by the landing gear using the following equation [Ref. 4]:

$$E_t = W_L N_g(\eta_t s_t + \eta_s s_s) \tag{A.1}$$

where:

W_L is the landing weight in pounds. 200 lbs was used.
N_g is the landing gear load factor.
η_t is the tire energy absorption efficiency.
s_t is the tire deflection.
η_s is the shock energy absorption factor.
s_s is the shock absorber deflection.

Using the following parameters:

landing weight = 200 lbs
touchdown speed = 5 ft/sec
number of main struts = 2
max static load per strut = 100 lbs
gear load factor = 3
Tire energy absorbtion efficiency = 0.47 Ref. 4, p54
shock Energy absorbtion efficiency = 0.50 Ref. 4, p54
maximum allowed tire deflection = 0.17 ft
required strut stroke = 0.10 ft

yields:

landing energy of A/C = 77.71 lb-ft
gear energy absorbtion = 78.25 lb-ft

To estimate the thickness of the main landing gear strut, the strut was treated as a spring leaf strut. The thickness was driven to provide the proper amount of strut stroke. From Ref. 6:

$$\Delta = \frac{Wl^3}{3EI} * \sec\theta \tag{A.2}$$

where:

Δ = strut deflection at the axle under 2 g impact load
W = aircraft weight, 200 lbs for this design
l = distance from axle to strut mounting point
E = modulus of elasticity
I = moment of inertia for cross section = width*thickness^3/12
θ = arctangent (l / height of strut)

The inputs were:

modulus of elasticity = 2,000,000 psi for fiberglass composite
distance from wheel to pivot point = 8 in
height of strut = 14.6 in
width of cross section = 6 in
thickness of cross section = 0.3 in
moment of inertia of cross section = 0.0135 in^4

which yielded:

strut deflection = 1.44 in or 0.12 ft

This value of strut deflection is close to the desired value. Based on this estimate, a thickness of 0.3-inches of fiberglass were used.

APPENDIX B: FINITE ELEMENT ANALYSIS OF MAIN LANDING GEAR

The following Matlab code was used to estimate the deflection of the main landing gear employing the methods of Reference 12. The main gear was divided into two sections and each section was analyzed separately. Figure B.1 defines the curved section with the applied maximum load and displacements defined. Figure B.2 defines the straight section with the applied maximum load and displacements defined.

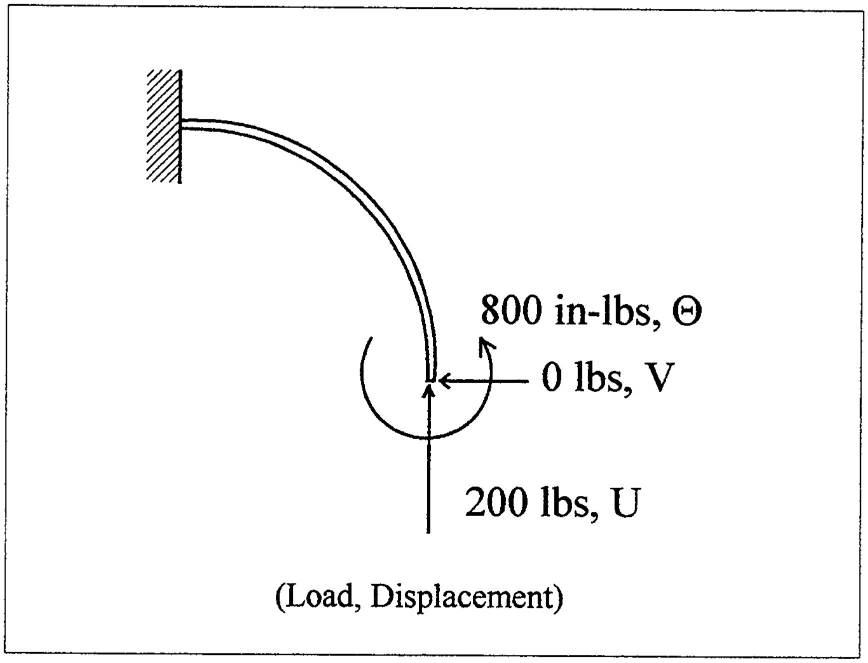

Figure B.1 Curved Section Model

```
% Landing Gear Finite Element Estimation
% Curved Section
beta = 9*pi/180; %radians
r = 8; % inches
E = 2000000; % psi  Composite
% cross section dimensions
w = 4.5; % in
t = .3; % in
I = w*(t^3)/12;
a = beta - sin(beta);
b = cos(beta)+((sin(beta))^2)/2 -1;
```

```
c = 3*beta/2 - 2*sin(beta) + (sin(2*beta))/4;
d = beta/2 - (sin(2*beta))/4;
e = cos(beta)-1;
K = [c b a; b d e; a e beta];
P = 200; % lbs
Q = 0; % lbs
M = 800; % in-lbs
def = r^2/(E*I)*K*[P*r; Q*r; M]
u = def(1)
v = def(2)
theta = def(3)/r*180/pi
```

Output:

width = 4.5 inches
thickness = 0.3 inches
deflections:
U = 0.0017 inches
V = -0.0315 inches
Θ = 2.8678 degrees

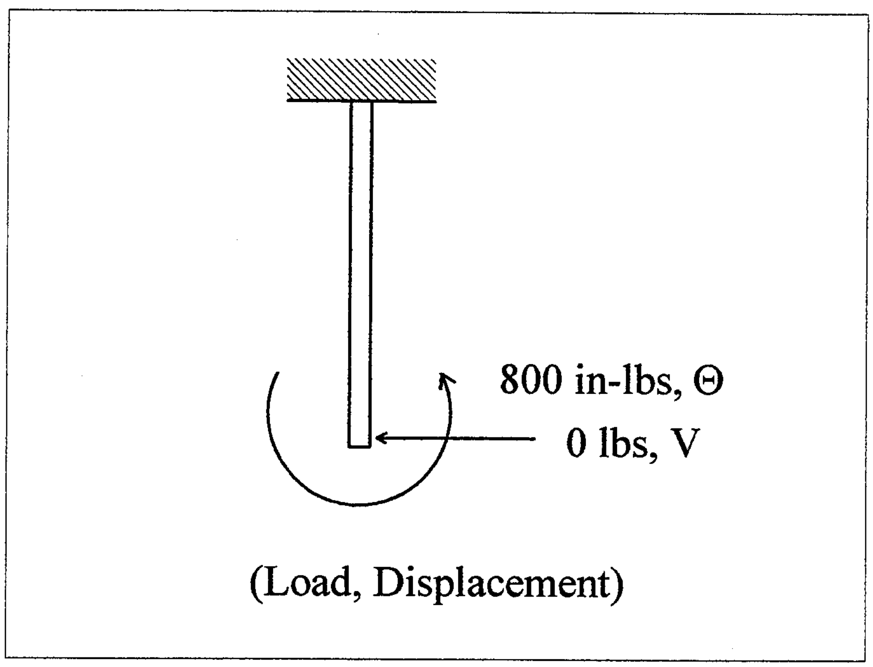

Figure B.2 Straight Section Model

```
% Landing Gear Finite Element Estimation
% Straight Section
E = 2000000; % psi  Composite
% cross section dimensions
w = 3 % in
t = .3 % in
L = 5.5; % inches
I = w*(t^3)/12;

K = (1/(E*I))*[(L^3)/3 (L^2)/2; (L^2)/2 L];
Y = 0 % lbs
M = 800 % in-lbs
def = K*[Y; M]
v = def(1)
theta = def(2)*180/pi
straight section
w = 3 in
t = .3 in
400 in-lbs moment
def =
   0.4481
   0.1630
```

Output:

V = 0.4481 inches

Θ = 9.3371 degrees

After superimposing the output values, it was apparent more structure was required. To reduce the deflections, a strut was added between the axle and mounting points. This strut appears on the final design.

APPENDIX C: MATLAB CODE USED TO SIZE HORIZONTAL TAIL

The following code was used to generate Figures 4.1 through 4.3. Reference 14 methods were utilized. Note: Reference 14 information is included in Reference 9.

```
% John Stewart, Blackbird Project
% HT.m  file to figure sensitivity
% of Wnsp and zeta to horiz tail params

% SPECIFIED DATA

WTO = 200;                % lbs
V = 168.78;               % ft/s = 100 kts
RHO = 0.002377;           % slug/ft^3 SSL
SOS = 1116.44;            % ft/s speed of sound
M = V/SOS;                % MACH Number
a = 2;                    % deg Angle of attack
m=WTO/32.17;              % slug Mass
Ixx =7.66;                % in^4  Mass Moment of Inertia
Iyy =16.23;               % in^4  Mass Moment of Inertia
Izz=22.9;                 % in^4  Mass Moment of Inertia
Ixz = 0;                  % in^4  Mass Moment of Inertia
thetanaut=0;
g=32.17;                  % gravity constant

% WIND TUNNEL DATA [Ref. 15]

A = 4.40;                 % aspect ratio
b = 138.0/12;             % ft wing span
S = 30.2;                 % ft^2 wing area
c = 32.3/12;              % ft  mean aerodynamic chord
a0 = -0.06;               % deg zero lift aoa
CLaWB = .8/10.01*180/pi;  % per radian
CM0WB = .012;
dCMdCL = -0.0475;
CD0 = 0.037;
l = 0.58;                         % taper ratio
Lc4 = 25.196;                     % deg sweep angle qtr chord wing
lC2 =  atan(tan(28*pi/180) - 2/A*((1-l)/(1+l)))*180/pi;
Xcg = 137.0;                      % fuselage station
XacW = (138.36 - 130.295)/12;     % wing aerodynamic center
XW = (138.36-Xcg)/12;             % dist from ac to cg
```

```
% Calculate dynamic pressure
qbar = .5*RHO*V^2;          % ft lbs

% Initialize storage vectors
ah = [];
wn = [];
zeta = [];
coefs=[];

% ** Begin Loop **

for AH = 1:1:6
for VH = .1:.05:.9

% HORIZONTAL TAIL

XH = (208 -Xcg)/12;          % ft dist from horiz ac and cg
LleH = 0.0;                  % deg sweep angle leading edge horiz tail
LteH = 0.0;                  % deg sweep angle of trailing edge horiz tail

SH = VH*S*c/XH;
bH = sqrt(AH*SH);

CtH = SH/bH - (bH/4*(tan(LleH*pi/180)+tan(LteH*pi/180)));
CrH = CtH + bH/2*(tan(LleH*pi/180)-tan(LteH*pi/180));

lH = CtH/CrH;                % horiz tail taper ratio

Lc2H = atan(tan(LleH*pi/180) - 2/AH*((1-lH)/(1+lH)))*180/pi;
Lc4H = atan(tan(LleH*pi/180) - 1/AH*((1-lH)/(1+lH)))*180/pi;

XacH = (208-130.295)/12;     % ft dist from c/4 wing to c/4 horiz tail
ZH = 19/12;                  % ft vert dist of horiz tail from wing
KA = 1/A - 1/(1+A^1.7);
Kl = (10 - 3*l)/7;
KH = (1-ZH/b)/(2*XH/b)^(1/3);
deda = 4.444*(KA*Kl*KH*(cos(Lc4*pi/180)^(0.5)))^1.19; % downwash
etaH = 1.0;                                         % horiz tail dyn press ratio
VH = XH*SH/(c*S);                                   % horiz tail volume

% CALCULATIONS
%(CRUISE CONDITIONS)
```

```
B = (1-M^2)^(.5);

CLaH = 2*pi*AH/(2+(AH^2*B^2/1*(1+(tan(Lc2H*pi/180))^2/B^2)+4)^(.5)); % per radian
CLa = CLaWB + ClaH*etaH*SH/S*(1-deda);                  % Per radian

CL = WTO/(.5*RHO*V^2*S);
CD = CD0 + CL^2/(pi*A*.85);
CMaWB = dCMdCL*CLaWB;
CMa = CMaWB;

CLqW = (A+2*cos(Lc4*pi/180))/(A*B+2*cos(Lc4*pi/180))*(.5+2*XW/c)*CLaWB;
CLqH = 2*CLaH*etaH*VH;
CLq = CLqW + CLqH;
K = 0.7;                              % FIG 5.1 Ref 14

CMqWM0 =
-K*CLaWB*cos(Lc4*pi/180)*(A*(2*(XW/c)^2+.5*XW/c)/(A+2*cos(Lc4*pi/180))+A^3
*(tan(Lc4*pi/180))^2/(24*(A+6*cos(Lc4*pi/180)))+1/8);

CMqW =
CMqWM0*((A^3*(tan(Lc4*pi/180))^2/(A*B+6*cos(Lc4*pi/180)))+3/B)/((A^3*(tan(Lc4
*pi/180))^2/(A+6*cos(Lc4*pi/180)))+3);

CMqH = -2*CLaH*etaH*VH*XH/c;
CMq = CMqW+CMqH;
CDa = 2*CL*CLa/(pi*A*.85);
CDad = 0;
CDU = 0;
CLU = (M^2)/(1-M^2)*CL;
CDq = 0;
CDad = 0;
CLad = 2*CLaH*etaH*VH*deda;
CMad =-2*CLaH*etaH*VH*XH/c*deda;

% Calculate Dimensional Derivatives

Za = -1*(CLa+CD)*qbar*S/m;            % ft/sec^2
Ma = CMa*qbar*S*c/Iyy;                % 1/sec^2
Mad = CMad*(c/(2*V))*qbar*S*c/Iyy;    % 1/sec
Mq = CMq*(c/(2*V))*qbar*S*c/Iyy;      % 1/sec

Wnsp = (Za*Mq/V - Ma)^(0.5);          % Short Period approximation
Zetasp = -(Mq + Za/V + Mad)/(2*Wnsp); % Short Period approximation
```

```
ah = [ah; AH VH bH SH CrH CtH];
wn = [wn; Wnsp];
zeta = [zeta; Zetasp];
coefs=[coefs;AH VH CLaH CLa CMa CMq CLad CMad Za Ma Mad Mq];
end
end

% plot for each aspect ratio
whitebg
figure(1)
plot(wn(1:17), ah(1:17,2),'r')
hold on
plot(wn(18:34), ah(18:34,2),'g')
plot(wn(35:51), ah(35:51,2),'b')
plot(wn(52:68), ah(52:68,2),'--r')
plot(wn(69:85), ah(69:85,2),'--g')
plot(wn(86:102), ah(86:102,2),'--b')
hold off
grid
title('Natural Frequency vs Tail Volume')
xlabel('Undamped Natural Frequency')
ylabel('Horizontal Tail Volume Coefficient')
%gtext('A=1')
%gtext('A=2')
%gtext('A=3')
%gtext('A=4')
%gtext('A=5')
%gtext('A=6')
%gtext('LE Sweep = 0 deg')

figure(2)
plot(zeta(1:17), ah(1:17,2),'r')
hold on
plot(zeta(18:34), ah(18:34,2),'g')
plot(zeta(35:51), ah(35:51,2),'b')
plot(zeta(52:68), ah(52:68,2),'--r')
plot(zeta(69:85), ah(69:85,2),'--g')
plot(zeta(86:102), ah(86:102,2),'--b')
hold off
title('Damping Ratio vs Tail Volume')
xlabel('Damping Ratio')
ylabel('Horizontal Tail Volume Coefficient')
grid
```

```
%gtext('A=1')
%gtext('A=2')
%gtext('A=3')
%gtext('A=4')
%gtext('A=5')
%gtext('A=6')
%gtext('LE Sweep = 0 deg')


figure(3)
plot(ah(1:17,6), ah(1:17,2),'r')
hold on
plot(ah(18:34,6), ah(18:34,2),'g')
plot(ah(35:51,6), ah(35:51,2),'b')
plot(ah(52:68,6), ah(52:68,2),'--r')
plot(ah(69:85,6), ah(69:85,2),'--g')
plot(ah(86:102,6), ah(86:102,2),'--b')
hold off
title('Horizontal Tail Tip Chord vs Tail Volume')
xlabel('Horizontal Tail Tip Chord, ft')
ylabel('Horizontal Tail Volume Coefficient')
grid
%gtext('A=1')
%gtext('A=2')
%gtext('A=3')
%gtext('A=4')
%gtext('A=5')
%gtext('A=6')
%gtext('LE Sweep = 0 deg')

figure(4)
plot(ah(1:17,5), ah(1:17,2),'r')
hold on
plot(ah(18:34,5), ah(18:34,2),'g')
plot(ah(35:51,5), ah(35:51,2),'b')
plot(ah(52:68,5), ah(52:68,2),'--r')
plot(ah(69:85,5), ah(69:85,2),'--g')
plot(ah(86:102,5), ah(86:102,2),'--b')
hold off
title('Horizontal Tail Root Chord vs Tail Volume')
xlabel('Horizontal Tail Root Chord, ft')
ylabel('Horizontal Tail Volume Coefficient')
```

```
grid
%gtext('A=1')
%gtext('A=2')
%gtext('A=3')
%gtext('A=4')
%gtext('A=5')
%gtext('A=6')
%gtext('LE Sweep = 0 deg')

figure(5)

plot(ah(1:17,3), ah(1:17,2),'r')
hold on
plot(ah(18:34,3), ah(18:34,2),'g')
plot(ah(35:51,3), ah(35:51,2),'b')
plot(ah(52:68,3), ah(52:68,2),'--r')
plot(ah(69:85,3), ah(69:85,2),'--g')
plot(ah(86:102,3), ah(86:102,2),'--b')
hold off
title('Horizontal Tail Span vs Tail Volume')
xlabel('Horizontal Tail Span, ft')
ylabel('Horizontal Tail Volume Coefficient')
grid
%gtext('A=1')
%gtext('A=2')
%gtext('A=3')
%gtext('A=4')
%gtext('A=5')
%gtext('A=6')
%gtext('LE Sweep = 0 deg')
%gtext('A=1')
%gtext('A=2')
%gtext('A=3')
%gtext('A=4')
%gtext('A=5')
%gtext('A=6')
%gtext('LE Sweep = 0 deg')

nalpha = qbar*S*CLa/WTO                    % g's per radian
```

APPENDIX D: DIGITAL DATCOM ANALYSIS

The Blackbird data was entered into the Digital Datcom using the format given in Reference 8. The input and output files are given below.

The program does not allow for the input of two vertical tails. To compensate for two vertical tails, a single tail was input using 80 percent of the total area. The 80 percent total area accounts for possible interference between the two tails.

The cruise flight condition of 100 knots velocity was used. To enhance the accuracy of the output, actual wind tunnel test data for the wing-body assembly was taken from Reference 15 and incorporated into the input file.

```
                    **************************************************
                    *  USAF STABILITY AND CONTROL  DIGITAL DATCOM   *
                    *  PROGRAM REV. JAN 91   DIRECT INQUIRIES TO:   *
                    *  WRIGHT LABORATORY  (WL/FIGC)  ATTN: W. BLAKE *
                    *     WRIGHT PATTERSON AFB, OHIO  45433         *
                    *  PHONE (513) 255-6764,  FAX (513) 258-4054    *
                    **************************************************
1            CONERR - INPUT ERROR CHECKING
0 ERROR CODES - N* DENOTES THE NUMBER OF OCCURENCES OF EACH ERROR
0 A - UNKNOWN VARIABLE NAME
0 B - MISSING EQUAL SIGN FOLLOWING VARIABLE NAME
0 C - NON-ARRAY VARIABLE HAS AN ARRAY ELEMENT DESIGNATION - (N)
0 D - NON-ARRAY VARIABLE HAS MULTIPLE VALUES ASSIGNED
0 E - ASSIGNED VALUES EXCEED ARRAY DIMENSION
0 F - SYNTAX ERROR

0****************************** INPUT DATA CARDS ******************************

 $FLTCON  NMACH=1.,
  MACH(1)=0.151,
  PINF = 14.7,
  TINF = 518.69,
  NALPHA=14.,
  ALPHA(1)=-4.1,-2.17,-0.17,1.85,3.83,5.82,7.83,9.83,11.84,13.84,15.85,
  17.84,19.86,21.87,
  WT=200.0,
  GAMMA=0.0,
 $END
 $OPTINS  ROUGFC=1.2E-3,
  SREF=4348.8,
  CBARR=32.26,
  BLREF=138.0,
 $END
 $SYNTHS
  XCG=137.,
  ZCG=0.,
  XW=113.626,
  ZW=0.18,
  ALIW=3.69,
```

```
 XH=204.5,
 ZH=19.,
 ALIH=0.0,
 XVF=193.5,
 ZVF=0.0,
$END
$BODY
 NX=9.,
 X(1)=91.9,94.4,100.6,111.28,121.75,133.36,144.23,159.35,168.93,
 S(1)=0.0,18.14,62.20,168.14,226.75,201.55,189.49,161.72,45.47,
 METHOD=1.,
 ELLIP=1.,
$END
$WGPLNF
 CHRDTP=22.,
 SSPNE=66.1,
 SSPN=76.6,
 CHRDR=40.,
 SAVSI=28.,
 CHSTAT=0.,
 TWISTA=-3.69,
 DHDADI=2.4,
 TYPE=1.,
$END
$EXPR01 CLAWB(1)=0.0799,CMAWB(1)=-0.00301,
 CDWB(1)=.0442,.0385,.0375,.0391,.0443,.0536,.0675,.0845,.1068,.1342,.1730,.218
 CLWB(1)=-.278,-.118,.053,.193,.364,.515,.661,.811,.953,1.072,1.194,1.264,1.327
 CMWB(1)=.0191,.016,.0098,-.0009,-.01,-.021,-.031,-.04,-.0465,-.049,-.056,-.061
$END
$HTPLNF
 CHRDTP=14.0,
 SSPNE=21.0,
 SSPN=21.0,
 CHRDR=14.,
 SAVSI=0.0,
 CHSTAT=0.,
 TWISTA=0.0,
 DHDADI=0.0,
 TYPE=1.0,
$END
$VTPLNF
 CHRDTP=22.4,
 SSPNE=19.0,
 SSPN=19.0,
 CHRDR=27.2,
 SAVSI=10.0,
 CHSTAT=0.,
 TYPE=1.,
$END
$SYMFLP
 FTYPE=1.0,
 NDELTA=8.0,
 DELTA(1)=5.0,10.0,15.0,20.0,-5.0,-10.0,-15.0,-20.0,
```

```
  PHETE=2.86E-4,
  PHETEP=2.75E-4,
  CHRDFI=5.,
  CHRDFO=5.,
  SPANFI=0.0,
  SPANFO=21.0,
 $END
NACA-W-5-23015-01
NACA-H-4-0012-01
NACA-V-4-0012-01
DAMP
DERIV RAD
DIM IN
CASEID AQUILA WING-BODY AND EMPENNAGE .35c ELEVATOR, 100 kts
NEXT CASE
1       THE FOLLOWING IS A LIST OF ALL INPUT CARDS FOR THIS CASE.
0
 $FLTCON  NMACH=1.,
 MACH(1)=0.151,
 PINF = 14.7,
 TINF = 518.69,
 NALPHA=14.,
 ALPHA(1)=-4.1,-2.17,-0.17,1.85,3.83,5.82,7.83,9.83,11.84,13.84,15.85,
 17.84,19.86,21.87,
 WT=200.0,
 GAMMA=0.0,
 $END
 $OPTINS  ROUGFC=1.2E-3,
 SREF=4348.8,
 CBARR=32.26,
 BLREF=138.0,
 $END
 $SYNTHS
 XCG=137.,
 ZCG=0.,
 XW=113.626,
 ZW=0.18,
 ALIW=3.69,
 XH=204.5,
 ZH=19.,
 ALIH=0.0,
 XVF=193.5,
 ZVF=0.0,
 $END
 $BODY
 NX=9.,
 X(1)=91.9,94.4,100.6,111.28,121.75,133.36,144.23,159.35,168.93,
 S(1)=0.0,18.14,62.20,168.14,226.75,201.55,189.49,161.72,45.47,
 METHOD=1.,
 ELLIP=1.,
 $END
 $WGPLNF
 CHRDTP=22.,
```

```
 SSPNE=66.1,
 SSPN=76.6,
 CHRDR=40.,
 SAVSI=28.,
 CHSTAT=0.,
 TWISTA=-3.69,
 DHDADI=2.4,
 TYPE=1.,
$END
$EXPR01 CLAWB(1)=0.0799,CMAWB(1)=-0.00301,
 CDWB(1)=.0442,.0385,.0375,.0391,.0443,.0536,.0675,.0845,.1068,.1342,.1730,.218
 CLWB(1)=-.278,-.118,.053,.193,.364,.515,.661,.811,.953,1.072,1.194,1.264,1.327
 CMWB(1)=.0191,.016,.0098,-.0009,-.01,-.021,-.031,-.04,-.0465,-.049,-.056,-.061
$END
$HTPLNF
 CHRDTP=14.0,
 SSPNE=21.0,
 SSPN=21.0,
 CHRDR=14.,
 SAVSI=0.0,
 CHSTAT=0.,
 TWISTA=0.0,
 DHDADI=0.0,
 TYPE=1.0,
$END
$VTPLNF
 CHRDTP=22.4,
 SSPNE=19.0,
 SSPN=19.0,
 CHRDR=27.2,
 SAVSI=10.0,
 CHSTAT=0.,
 TYPE=1.,
$END
$SYMFLP
 FTYPE=1.0,
 NDELTA=8.0,
 DELTA(1)=5.0,10.0,15.0,20.0,-5.0,-10.0,-15.0,-20.0,
 PHETE=2.86E-4,
 PHETEP=2.75E-4,
 CHRDFI=5.,
 CHRDFO=5.,
 SPANFI=0.0,
 SPANFO=21.0,
$END
NACA-W-5-23015-01
NACA-H-4-0012-01
NACA-V-4-0012-01
DAMP
DERIV RAD
DIM IN
CASEID AQUILA WING-BODY AND EMPENNAGE .35c ELEVATOR, 100 kts
NEXT CASE
```

0 INPUT DIMENSIONS ARE IN IN, SCALE FACTOR IS 1.0000
AUTOMATED STABILITY AND CONTROL METHODS PER APRIL 1976 VERSION OF DATCOM
WING SECTION DEFINITION
0 IDEAL ANGLE OF ATTACK = 0.80042 DEG.
ZERO LIFT ANGLE OF ATTACK = -2.33364 DEG.

IDEAL LIFT COEFFICIENT = 0.36873

ZERO LIFT PITCHING MOMENT COEFFICIENT = -0.05944

MACH ZERO LIFT-CURVE-SLOPE = 0.11440 /DEG.
LEADING EDGE RADIUS = 0.00000 FRACTION CHORD

MAXIMUM AIRFOIL THICKNESS = 0.15000 FRACTION CHORD

DELTA-Y = 6.66591 PERCENT CHORD

0 MACH= 0.1510 LIFT-CURVE-SLOPE = 0.11507 /DEG. XAC = 0.23305
AUTOMATED STABILITY AND CONTROL METHODS PER APRIL 1976 VERSION OF DATCOM
HORIZONTAL TAIL SECTION DEFINITION
0 IDEAL ANGLE OF ATTACK = 0.00000 DEG.

ZERO LIFT ANGLE OF ATTACK = 0.00000 DEG.

IDEAL LIFT COEFFICIENT = 0.00000
ZERO LIFT PITCHING MOMENT COEFFICIENT = 0.00000

MACH ZERO LIFT-CURVE-SLOPE = 0.11054 /DEG.

LEADING EDGE RADIUS = 0.00000 FRACTION CHORD

MAXIMUM AIRFOIL THICKNESS = 0.12000 FRACTION CHORD

DELTA-Y = 5.33297 PERCENT CHORD

0 MACH= 0.1510 LIFT-CURVE-SLOPE = 0.11140 /DEG. XAC = 0.24012
AUTOMATED STABILITY AND CONTROL METHODS PER APRIL 1976 VERSION OF DATCOM
VERTICAL TAIL SECTION DEFINITION
0 IDEAL ANGLE OF ATTACK = 0.00000 DEG.
ZERO LIFT ANGLE OF ATTACK = 0.00000 DEG.

IDEAL LIFT COEFFICIENT = 0.00000

ZERO LIFT PITCHING MOMENT COEFFICIENT = 0.00000

MACH ZERO LIFT-CURVE-SLOPE = 0.11083 /DEG.

LEADING EDGE RADIUS = 0.00000 FRACTION CHORD
MAXIMUM AIRFOIL THICKNESS = 0.12000 FRACTION CHORD
DELTA-Y = 5.33265 PERCENT CHORD
0 MACH= 0.1510 LIFT-CURVE-SLOPE = 0.11170 /DEG. XAC = 0.23988

AUTOMATED STABILITY AND CONTROL METHODS PER APRIL 1976 VERSION OF DATCOM
CHARACTERISTICS AT ANGLE OF ATTACK AND IN SIDESLIP
WING-BODY-VERTICAL TAIL-HORIZONTAL TAIL CONFIGURATION
AQUILA WING-BODY AND EMPENNAGE .35c ELEVATOR, 100 kts

FLIGHT CONDITIONS							REFERENCE DIMENSIONS				
MACH NUM	ALT	VEL	PRESS	TEMP	REYN No	REF. AREA	REF LONG.	LEN LAT.	MOM HORIZ	REF. CENTER VERT	
	IN	IN/SEC	LB/IN^2	DEG R	1/FT	IN**2	IN	IN	IN	IN	
0.151		2022.82	14.7	518.69	1067500	4348.8	32.26	138	137	0	

							DERIVATIVE (PER RADIAN)				
ALPHA	CD	CL	CM	CN	CA	XCP	CLA	CMA	CYB	CNB	CLB
-4.1	0.049	-0.31	0.096	-0.315	0.027	-0.31	4.772	-0.64	-0.257	-0.206	0.02624
-2.2	0.042	-0.15	0.079	-0.147	0.037	-0.53	5.013	-0.56			-0.0099
-0.2	0.041	0.03	0.058	0.032	0.041	1.837	4.616	-0.64			-0.04839
1.8	0.042	0.178	0.034	0.179	0.036	0.188	4.634	-0.66			-0.08125
3.8	0.047	0.355	0.012	0.357	0.023	0.03	4.811	-0.65			-0.1196
5.8	0.056	0.511	-0.01	0.514	0	0	4.42	-0.67			-0.1542
7.8	0.071	0.663	-0.04	0.666	-0.02	-0.1	4.425	-0.71			-0.188
9.8	0.089	0.821	-0.06	0.824	-0.05	-0.1	4.409	-0.76			-0.2223
11.8	0.114	0.972	-0.09	0.974	-0.09	-0.1	3.988	-0.73			-0.2549
13.8	0.144	1.1	-0.113	1.102	-0.123	-0.1	3.733	-0.82			-0.283
15.9	0.187	1.233	-0.145	1.237	-0.157	-0.12	3.114	-1.06			-0.3115
17.8	0.238	1.318	-0.186	1.327	-0.177	-0.14	2.347	20.47			-0.3304
19.9	0.206	1.397	1.31	1.384	-0.281	0.947	-5.049	19.53			-0.3474
21.9	0.17	0.965	1.1956	0.959	-0.202	1.247	-19.57	-26.1			-0.2731

ALPHA	Q/QINF	EPSLON	D(EPSLON)/D(ALPHA)
-4.1	1	0.242	0.565
-2.2	1	1.332	0.578
-0.2	1	2.514	0.604
1.8	1	3.759	0.627
3.8	1	5.022	0.644
5.8	1	6.316	0.639
7.8	1	7.577	0.573
9.8	1	8.613	0.471
11.8	1	9.467	0.394
13.8	1	10.193	0.297
15.9	1	10.655	0.058
17.8	1	10.431	-0.302
19.9	1	9.431	-0.235
21.9	1	9.48	0.025

0*NOTE* OUTPUT REFLECTS EXPERIMENTAL DATA INPUTS

AUTOMATED STABILITY AND CONTROL METHODS PER APRIL 1976 VERSION OF DATCOM
CHARACTERISTICS AT ANGLE OF ATTACK AND IN SIDESLIP
WING-BODY-VERTICAL TAIL-HORIZONTAL TAIL CONFIGURATION
AQUILA WING-BODY AND EMPENNAGE .35c ELEVATOR, 100 kts

---- FLIGHT CONDITIONS ----							---- REFERENCE DIMENSIONS ----				
MACH NUM	ALT	VEL	PRESS	TEMP	REYN No	REF. AREA	REF LONG.	LEN LAT.	MOM HORIZ	REF. CENTER VERT	
	IN	IN/SEC	LB/IN^2	DEG R	1/FT	IN**2	IN	IN	IN	IN	
0.151		2022.82	14.7	518.69	1067500	4348.8	32.26	138	137	0	

DYNAMIC DERIVATIVES (PER RADIAN)

-------PITCHING-------			-----ACCELERATION------		-----ROLLING-----			-----YAWING-----	
ALPHA	CLQ	CMQ	CLAD	CMAD	CLP	CYP	CNP	CNR	CLR
-4.1	5.74	-5.499	1.118	-2.475	-0.4943	-0.031	0.0295	-0.3453	0.0007
-2.17			1.143	-2.531	-0.5129	-0.046	0.0378	-0.3473	0.02917
-0.17			1.194	-2.644	-0.5313	-0.063	0.0501	-0.3524	0.06031
1.85			1.241	-2.748	-0.5468	-0.083	0.0649	-0.3612	0.09311
3.83			1.274	-2.82	-0.5587	-0.1019	0.0803	-0.3733	0.1263
5.82			1.264	-2.799	-0.5396	-0.11	0.0802	-0.3892	0.1602
7.83			1.133	-2.509	-0.4533	-0.086	0.0365	-0.4062	0.1902
9.83			0.9327	-2.065	-0.3425	-0.036	-0.034	-0.4191	0.2096
11.84			0.7791	-1.725	-0.2326	0.0299	-0.1105	-0.4271	0.2207
13.84			0.5868	-1.299	-0.1502	0.0863	-0.1709	-0.4279	0.2216
15.85			0.1145	-0.2534	0.2362	0.7068	-0.3189	-0.4253	0.2187
17.84			-0.5982	1.324	0.5359	-1.549	-0.9007	-0.3822	0.1562
19.86			-0.4643	1.028	0.4136	-0.7036	-0.5478	-0.3493	0.104
21.87			0.0485	-0.1073	0.2989	-0.4964	-0.4203	-0.324	0.06171

*** VEHICLE WEIGHT = 200.00 LB.
*** LEVEL FLIGHT LIFT COEFFICIENT = 0.19602

---------INCREMENTS DUE TO DEFLECTION--------- ---DERIVATIVES (PER DEGREE)---

DELTA	D(CL)	D(CM)	D(CL MAX)	D(CD MIN)	(CLA)D	(CH)A	(CH)D
5	0.028	-0.05	0.02	0.001	NDM	0	-0.01
10	0.055	-0.11	0.04	0.002	NDM		-0.01
15	0.079	-0.158	0.06	0.004	NDM		-0.01
20	0.085	-0.171	0.07	0.006	NDM		-0.01
-5	-0.03	0.055	0.02	0.001	NDM		-0.01
-10	-0.06	0.1097	0.04	0.002	NDM		-0.01
-15	-0.08	0.1578	0.06	0.004	NDM		-0.01
-20	-0.09	0.1708	0.07	0.006	NDM		-0.01

0 *** NOTE * HINGE MOMENT DERIVATIVES ARE BASED ON TWICE THE AREA-MOMENT OF THE CONTROL ABOUT ITS HINGE LINE

--------- INDUCED DRAG COEFFICIENT INCREMENT , D(CDI) , DUE TO DEFLECTION ---------

DELTA =

ALPHA	5.0	10.0	15.0	20.0	-5.0	-10.0	-15.0	-20.0	
-4.1	0	0	0.001	0	0.0014	0.0038	0.0066	0.007	
-2.2	0	0	0.0017	0	0.0012	0.0033	0.006	0.007	
-0.2	0	0.001	0.0024	0	0.001	0.0029	0.0053	0.006	
1.8	0	0.0013	0.003	0	0.001	0.0024	0.0047	0.005	
3.8	0	0.0017	0.0036	0	0.001	0.002	0.0041	0.005	
5.8	0.001	0.0021	0.0041	0	0	0.0017	0.0036	0.004	
7.8	0.001	0.0025	0.0047	0.01	0	0.0012	0.003	0.003	
9.8	0.001	0.003	0.0055	0.01	0	0.001	0.0022	0.003	
11.8	0.0014	0.0036	0.0064	0.01	0	0	0.0013	0.002	
13.8	0.0017	0.0044	0.0074	0.01	0	0	0	0	
15.9	0.0021	0.0052	0.0087	0.01	-0.001	-0.002	-0.001	0	
17.8	0.0028	0.0064	0.0104	0.012	-0.002	-0.003	-0.003	0	
19.9	0.0036	0.0081	0.0129	0.014	-0.003	-0.004	-0.005	-0.01	
21.9	0.0041	0.0092	0.0144	0.016	-0.003	-0.006	-0.007	-0.01	

0***NDM PRINTED WHEN NO DATCOM METHODS EXIST

1 THE FOLLOWING IS A LIST OF ALL INPUT CARDS FOR THIS CASE.

0

1 END OF JOB.

At the design weight and design cruise condition, the following values were extracted from the output:

α	1.85
C_D	0.042
C_L	0.178
C_M	0.034
C_N	0.179
C_A	0.036
X_{CP}	0.188
$C_{L\alpha}$	4.634
$C_{M\alpha}$	-0.66
$C_{y\beta}$	-0.257
$C_{n\beta}$	-0.206
$C_{l\beta}$	-0.08125
C_{lq}	5.74
C_{Mq}	-5.499
$C_{L\alpha}$	1.241
$C_{M\alpha}$	-2.748
C_{lp}	-0.5468
C_{yp}	-0.083
C_{np}	0.0649
C_{nr}	-0.3612
C_{lr}	0.09311

Table D.1 Cruise Digital Datcom Data

This data was compared to the results from the methods of Reference 14. There are discrepancies between the two sets of data. Since both sets of data are based on the same method, further analysis is required, which is beyond the scope of this project.

APPENDIX E: TAIL BOOM CONFIGURATIONS

The following data were taken from Reference 12 with some modifications. The yield was calculated on a spreadsheet using:

$$\sigma = \frac{My}{I} \tag{E.1}$$

from Reference 11.

Config-uration	Material	O.D. (in)	Thickness (in)	Mean Radius (in)	I (in^4)	My/I (psi)	Density (lb/cu in)	Weight (lb/ft)	Total Weight 2 Booms (lbs)
1	2024-T3	1.5	0.049	0.7255	0.0588	67818.30	0.1	0.2680	2.50
2	2024-T3	1.5	0.065	0.7175	0.0754	52270.98	0.1	0.3516	3.28
3	2024-T3	1.5	0.25	0.625	0.1917	17910.92	0.1	1.1781	11.00
4	2024-T3	1.5	0.5	0.5	0.1964	13992.90	0.1	1.8850	17.59
5	2024-T3	1.75	0.25	0.75	0.3313	12438.14	0.1	1.4137	13.19
6	2024-T3	1.875	0.065	0.905	0.1514	32855.44	0.1	0.4435	4.14
7	6061-T6	1.5	0.035	0.7325	0.0432	93139.63	0.098	0.1894	1.77
8	6061-T6	1.5	0.049	0.7255	0.0588	67818.30	0.098	0.2627	2.45
9	6061-T6	1.5	0.058	0.721	0.0683	58012.20	0.098	0.3090	2.88
10	6061-T6	1.5	0.065	0.7175	0.0754	52270.98	0.098	0.3446	3.22
11	6061-T6	1.5	0.125	0.6875	0.1276	29604.82	0.098	0.6350	5.93
12	6061-T6	1.625	0.058	0.7835	0.0876	49126.05	0.098	0.3358	3.13
13	6061-T6	1.75	0.035	0.8575	0.0693	67964.41	0.098	0.2218	2.07
14	6061-T6	1.75	0.049	0.8505	0.0947	49348.40	0.098	0.3079	2.87
15	6061-T6	1.75	0.058	0.846	0.1103	42135.59	0.098	0.3626	3.38
16	6061-T6	1.875	0.058	0.9085	0.1366	36537.60	0.098	0.3893	3.63
17	6061-T6	2	0.065	0.9675	0.1849	28747.66	0.098	0.4647	4.34

Table E.1 Configuration Data

INITIAL DISTRIBUTION LIST

		No. Copies
1.	Defense Technical Information Center Cameron Station Alexandria, VA 22304-6145	2
2.	Library, Code 52 Naval Postgraduate School Monterey, CA 93943-5101	2
3.	Chairman, Code AA Naval Postgraduate School Monterey, CA 93943-5000	1
4.	Professor Richard M. Howard, Code AA/Ho Naval Postgraduate School Monterey, CA 93943-5100	3
5.	Professor Conrad F. Newberry, Code AA/Ne Naval Postgraduate School Monterey, CA 93943-5100	1
6.	Mr. Don Meeks, Code AA Naval Postgraduate School Monterey, CA 93943-5100	1
7.	LT John E.C. Stewart Operations Department USS Theodore Roosevelt (CVN-71) FPO AE 09599-2871	1
8.	Mr. William C. Drake, Jr. Lockheed Missiles & Space Company, Inc. 16020 Empire Grade Rd. Santa Cruz, CA 95060	1
9.	Mrs. June Stewart 368 Park Ave. Wheeling, IL 60090	1

10. Mr. Phillip Robinson 1
111 S. Baybrook #205
Palatine, IL 60067